

VIBRATION TESTING OF THE CONSTELLATION X  
SPECTROSCOPY X-RAY TELESCOPE REFLECTOR  
MOUNTING DESIGN

by

Joshua Schneider

B.S. in Aeronautical Engineering, June 2004, United States Air Force Academy

A Thesis submitted to

The Faculty of

The School of Engineering and Applied Science  
of The George Washington University in partial satisfaction  
of the requirement for the degree of Master of Science

24 September, 2005

Thesis directed by

Shahram Sarkani

Professor of Engineering Management and Systems Engineering

# Report Documentation Page

Form Approved  
OMB No. 0704-0188

Public reporting burden for the collection of information is estimated to average 1 hour per response, including the time for reviewing instructions, searching existing data sources, gathering and maintaining the data needed, and completing and reviewing the collection of information. Send comments regarding this burden estimate or any other aspect of this collection of information, including suggestions for reducing this burden, to Washington Headquarters Services, Directorate for Information Operations and Reports, 1215 Jefferson Davis Highway, Suite 1204, Arlington VA 22202-4302. Respondents should be aware that notwithstanding any other provision of law, no person shall be subject to a penalty for failing to comply with a collection of information if it does not display a currently valid OMB control number.

1. REPORT DATE <b>24 SEP 2005</b>		2. REPORT TYPE <b>N/A</b>		3. DATES COVERED <b>-</b>	
4. TITLE AND SUBTITLE <b>Vibration Testing Of The Constellation X Spectroscopy X-Ray Telescope Reflector Mounting Design</b>				5a. CONTRACT NUMBER	
				5b. GRANT NUMBER	
				5c. PROGRAM ELEMENT NUMBER	
6. AUTHOR(S)				5d. PROJECT NUMBER	
				5e. TASK NUMBER	
				5f. WORK UNIT NUMBER	
7. PERFORMING ORGANIZATION NAME(S) AND ADDRESS(ES) <b>The George Washington University</b>				8. PERFORMING ORGANIZATION REPORT NUMBER	
9. SPONSORING/MONITORING AGENCY NAME(S) AND ADDRESS(ES)				10. SPONSOR/MONITOR'S ACRONYM(S)	
				11. SPONSOR/MONITOR'S REPORT NUMBER(S)	
12. DISTRIBUTION/AVAILABILITY STATEMENT <b>Approved for public release, distribution unlimited</b>					
13. SUPPLEMENTARY NOTES <b>The original document contains color images.</b>					
14. ABSTRACT					
15. SUBJECT TERMS					
16. SECURITY CLASSIFICATION OF:			17. LIMITATION OF ABSTRACT <b>UU</b>	18. NUMBER OF PAGES <b>72</b>	19a. NAME OF RESPONSIBLE PERSON
a. REPORT <b>unclassified</b>	b. ABSTRACT <b>unclassified</b>	c. THIS PAGE <b>unclassified</b>			

## **ABSTRACT**

This paper covers the results of four vibration tests performed on the Constellation X Spectroscopy X-Ray Telescope Mirrors. The testing provided critical understanding of the glass strength when subjected to high level vibration loads and helped determine the resonance frequencies of the mirror when mounted using ten grooves in a titanium strut. The data from this testing indicates that the Schott D-263 glass mirrors meets the requirements for glass set forth in the NASA Technical Standard 5001. This is a critical step forward to ensure the success of the Constellation X mission.

Four objectives were achieved from this testing. A finite element model successfully predicted the natural frequency of the mirrors during sine sweeps. The testing determined that the D-263 glass can survive loads seen during launch. The third and fourth objectives, collecting data for mirror and fixture's response characteristics to use as baseline of future designs, were also achieved.

The most important result from this series of tests indicates that the mirrors are capable of surviving the launch environment of a Delta IV Heavy or Atlas 5. All of the D-263 glass mirrors survived, at a minimum, a sine burst loading of 90 gn at 90 Hz. The mirrors clearly passed vibration requirement and do not represent any major hindrance for use in the SXT Constellation X telescope.

The views expressed in this article are those of the author and do not reflect the official policy or position of the United States Air Force, Department of Defense, or the U.S. Government.

## **ACKNOWLEDGEMENTS**

It needs to be mentioned that this thesis could not have been completed without the support of many people at George Washington University and NASA Goddard Space Flight Center. Dr. Sarkani of George Washington University provided critical guidance and direction throughout the thesis process.

At NASA Goddard, the Constellation X Spectroscopy X-Ray Telescope Mechanical Systems Engineering Team was critical to the success of this work. Jeff Stewart (GSFC-543), Lt Andrew Carlson (USAF), Burt and Janet Squires (Swales), and Chris Kolos (GSFC-547) all provided valuable help along the way. Outside of SXT team, Onur Atabak and Kai Chan Wing provided additional support during my time at GSFC. Dr Arun Varshney of Alfred University also provided invaluable understanding of glass properties and strengthening techniques.

# TABLE OF CONTENTS

	<u>Page</u>
ABSTRACT.....	ii
ACKNOWLEDGEMENTS.....	iii
TABLE OF CONTENTS.....	iv
LIST OF FIGURES .....	vi
LIST OF TABLES.....	viii
LIST OF ACRONYMS .....	ix
GLOSSARY .....	xi
CHAPTER 1: Introduction .....	1
1.1 Review of Literature .....	1
1.2 Chapter Summary .....	2
1.3 Statement of Purpose .....	3
CHAPTER 2: Background.....	5
2.1 Mission Overview.....	5
2.2 Science Goals.....	5
2.3 Mission Design .....	7
2.4 Constellation X Telescope Design.....	9
2.5 Optical Assembly Pathfinders.....	13
2.6 Glass Properties .....	16
2.7 Schott Desag 263 Glass Properties .....	21
2.8 Constellation X SXT Slumping Process.....	22
2.9 Strength Testing.....	23
2.9.1 Strength Test Results from 1999 Biaxial Test.....	26
2.9.2 Strength Test Results from 2003 Bending Test .....	26
2.9.3 Strength Test Results from 2004 Biaxial Tests.....	28
2.9.4 Strength Test Results from 2005 Biaxial Tests.....	30
2.9.5 Strength Test Results from Chemically Strengthened Glass .....	32
2.10 Finite Element Modeling of Launch Loads .....	35
2.11 Vibration Test 2004 .....	36
2.12 Flight-Like Vibration Test.....	38
CHAPTER 3: Problem Statement.....	41
3.1 Statement of Purpose .....	41
3.2 Test Matrix.....	42

3.3 Vibration Testing Equipment and Setup.....	43
3.4 Finite Element Analysis Modeling .....	47
CHAPTER 4: Results and Analysis.....	50
4.1 Mirror 489 P-80 .....	51
4.2 Mirror 489 P-90 .....	51
4.3 Mirror 489 P-88 .....	51
4.4 Mirror Comparison .....	52
CHAPTER 5: Conclusions and Recommendations.....	55
REFERENCES .....	58

## LIST OF FIGURES

	<u>Page</u>
FIGURE 2.1: Positioning of Constellation X at L2 .....	8
FIGURE 2.2: Constellation X Launch Configuration for 2 Observatories .....	9
FIGURE 2.3: Constellation X Baseline Design.....	10
FIGURE 2.4: X-Ray Reflection Path and Detection Devices .....	10
FIGURE 2.5: SXT Mirror Buildup.....	12
FIGURE 2.6: SXT Mirror Housing .....	12
FIGURE 2.7: Optical Assembly Pathfinder 1.....	14
FIGURE 2.8: a) Optical Assembly Pathfinder 2 b) OAP2 nested within OAP1.....	15
FIGURE 2.9: Volume-Temperature Plot for Glass Forming Material.....	17
FIGURE 2.10 Biaxial Strength Testing Setup.....	23
FIGURE 2.11 FEA Model for Biaxial Strength Testing for 1 Quadrant.....	24
FIGURE 2.12: Bending Strength Testing Setup.....	25
FIGURE 2.13: FEA Results for Bending Tests .....	25
FIGURE 2.14: Results from 1999 Strength Tests .....	26
FIGURE 2.15: Load Displacement Curves for Glass Shell Strength Tests.....	27
FIGURE 2.16: Constellation X Slumped Shell Strength Comparison .....	28
FIGURE 2.17: Strength Comparison of four Schott D-263 Glass Deliveries .....	29
FIGURE 2.18: Glass Strength Comparison between Deliveries and Cleaning.....	30
FIGURE 2.19: D-263 Strength Comparisons .....	31
FIGURE 2.20: Typical Particle Contamination found in D-263 Glass .....	32
FIGURE 2.21: Strengthened D-263 Glass Strength Comparison.....	34

FIGURE 2.22: D-263 Failure Due to an Edge Defect.....	35
FIGURE 2.23: 2004 Vibration Setup.....	37
FIGURE 2.24: Sine Sweep from 2004 Vibration Test .....	38
FIGURE 3.1: Vibration Fixture and Housing.....	44
FIGURE 3.2: Laser Vibrometer Measurement Position on Mirror .....	46
FIGURE 3.3: Accelerometer Positions.....	47
FIGURE 3.4: Finite Element Model .....	48
FIGURE 3.5: First Mode Prediction from FEA Model at 168 Hz.....	48
FIGURE 3.6: FEA Model Prediction of Highest Stress .....	49
FIGURE 4.1: Typical Sine Burst Response for the Sine Burst Tests.....	50
FIGURE 4.2: Pre and Post Sine Sweep Comparison.....	52
FIGURE 4.3: Sine Sweep Data at First Resonance Frequency .....	53
FIGURE 4.4: Sine Sweep Response over 10-500 Hz for All Mirrors.....	54

**LIST OF TABLES**

	<u>Page</u>
TABLE 2.1 SXT Mirror Requirements [10].....	11
TABLE 2.2 Schott Desag 263 Glass Properties [15].....	21
TABLE 3.1 Test Matrix for Vibration Test.....	43

## LIST OF ACRONYMS

CCD	Charge Coupled Device
Con-X	Constellation X
CTE	Coefficient of Thermal Expansion
DVC	Digital Vibration Controller
ELV	Expendable Launch Vehicle
FEA	Finite Element Analysis
FEM	Finite Element Model
FS	Factor of Safety
GEVS	General Environmental Verification Specification
GSFC	Goddard Space Flight Center
H	Hyperbolic (Secondary) Mirror
HXT	Hard X-Ray Telescope (High Energy)
LDS	Ling Dynamic Systems
L2	Lagrange Point 2
MS	Margin of Safety
NASA	National Aeronautics and Space Administration
OAP	Optical Pathfinder Assembly
P	Primary (Parabolic) Mirror
RFC	Reflection Focal Plane Camera
RGS	Reflection Grating Spectrometer
RMS	Root Mean Squared
S	Secondary (Hyperbolic)

SAO	Smithsonian Astrophysical Observatory
SRC	Spectroscopy Readout Camera
SXT	Soft (Spectroscopy) X-Ray Telescope
T	Temperature
TLL	Test Limit Load
TRIP	Technology Readiness and Implementation Plan
XMS	X-Ray Microcalorimeter Spectrometer
ZOC	Zero Order Camera

## **GLOSSARY**

Acoustic Loads	- Loads caused by pressure variations generated by the noise of launch vehicle
Annealing Point	- At this temperature stresses in the glass become are relaxed
Atlas V	- Heavy lift rocket built and designed by Lockheed Martin Corp.
Delta	- Change in a particular property
Delta IV Heavy	- Heavy lift rocket built and designed by Boeing Corp.
Fatigue	- Reduction of material strength due to time under stress. May result from many factors.
Fundamental Frequency	- The natural frequency of an item, also where the first mode of the item occurs when undergoing sine sweeps.
Glass Strength	- Load at which the glass will fail; dependent upon many variables such as treatment, manufacturing process, handling, humidity, and load application. It is usually measured in ksi or MPa.
Glass Substrate	- Glass that has been formed to the proper shape but not coated with any reflective material
Hyperbolic Reflector	- Secondary reflector. X-rays graze off of the secondary mirror before reaching the detectors. See Secondary Reflector.
Low Frequency	- Frequency range from 0 to 150 Hz covered in a sine sweep.
Mirror	- Constellation X reflector
Parabolic Reflector	- X-rays graze off of the mirror before reaching the secondary mirror. Also see Primary Reflector

Primary Reflector	- Mirror with a prescription defined by a parabolic equation. Also see Parabolic Reflector.
Replication	- Process of taking a formed reflector and applying a thin coating of gold to the glass shell to enhance surface qualities.
Reflector	- A piece of D-263 glass that has been slumped, cut and coated to the proper specifications for the soft x-ray telescope (SXT).
Secondary Reflector	- Mirror with a prescription defined by a hyperbolic equation. Also see Hyperbolic Reflector.
Sine Burst	- Used to ensure the structural integrity of spacecraft components, also used to determine the failure point under quasi-static loading. Drive signal is in the shape of a sine wave.
Sine Sweep	- A vibration testing technique where the drive frequency is increased from a low value to a higher value (typically from 10 Hz-2000Hz) to determine resonance frequencies for the test item. Drive signal is a sine wave.
Slumping	- Heating glass to a temperature where it takes the shape of the mandrel it is laid on.
Strain Point	- Stresses formed in glass above this temperature will be permanent once the glass is cooled
Structural Loads	- Loads resulting from how an object is held, such as a mirror mounting, and stresses applied through the structure including vibrations.

# **CHAPTER 1: INTRODUCTION**

The Constellation X mission is critical to the future of NASA's goal to explore and understand the universe. The space based X-ray telescope is slated to launch in 2017 and will collect X-ray light emitted from matter throughout the universe. A critical component of the telescope design is the Spectroscopy X-ray Telescope (SXT). It is vital to the success of the mission to determine the survivability of the mirrors used to collect X-rays in the SXT. The mirrors are made of Schott D-263 glass and earlier strength testing indicates that the mirrors may be unable to withstand the launch loads. This thesis covers the vibration testing of three Constellation X mirrors. The vibration tests have four objectives; determine survivability of glass, correlate analytic models, understand glass properties in a quasi-static environment, and evaluate the baseline mirror-fixture design.

## **1.1 Review of Literature**

Earlier vibration test plans and summaries provided initial information on developing the testing for the glass substrates and mounting scheme. These alone were inadequate to understand all of the unique aspects of this testing. NASA's Constellation-X homepage provides a great deal of information covering all aspects of the mission; including engineering and science characteristics as the Constellation X design is updated [1].

Thompson was extremely helpful developing an understanding of the theory of vibrations [2]. His text contains a wide overview of vibration theory and application using computational techniques. NASA's Preferred Reliability Practices provides a review of NASA Goddard Space Flight Center's technique for using a sine burst to apply quasi-static loads [3].

Due to the nature of glass, a large portion of time was spent understanding glass properties, particularly with respect to mechanical and thermal properties. Varshneya provides an exceptional overview of the glass properties and techniques for strengthening [4]. Current glass processing and strengthening technologies are also overviewed extensively in Uhlmann and Kreidl [5]. Carlson's paper provided a broad review of the previous vibration and strength testing in Constellation X until 2004[6].

## **1.2 Chapter Summary**

Chapter 1 covers the brief introduction into this thesis followed by a review of the literature used in preparation for this paper. Chapter two covers an extensive background of information on the Constellation X design, including glass properties and glass strength testing. This provides the reader with an understanding of the current status of the Constellation X mission and SXT mirrors.

A comprehensive review of the testing methods and equipment is discussed in Chapter 3. This also includes the failure predictions using a finite element analysis. Chapter 3 also includes a brief discussion of challenges that developed during testing and resulting resolutions. Within Chapter 4, results and analysis from testing are presented. Results from the testing are also compared to four objectives for the test.

In the final chapter, a brief summary of the Constellation X vibration testing is presented along with a full discussion of the implications on the Constellation X mission. This chapter also includes a discussion of the future direction of the vibration testing and recommendations for modifying the current equipment to gather more data.

### 1.3 Statement of Purpose

This thesis focuses on the initial vibration testing of the Constellation X Spectroscopy X-ray Telescope baseline mounting design. The SXT mirrors are approximately 8" x 7.5" and are 400 microns thick (0.01575"). The mirrors are bonded by epoxy at five points on top and bottom in a 3 mil groove machined into a titanium strut. The mirrors must be capable of surviving launch loads when mounted in this position. The vibration test is focused on achieving four major goals. Below is a discussion of the four objectives for this vibration testing:

1. Validation of the survivability of glass throughout the launch environment. The Constellation X telescopes will be launched on an Atlas V or Delta IV Heavy launch vehicle. Both of these vehicles create a strong acoustic loads and structural loads during the initial launch and as they pass through Mach 1, approximately 1000 ft/sec.
2. Understanding of D-263 glass properties under quasi-static loads. While the strength of the glass has been determined using ring-on-ring bi-axial tests and bending test, additional test simulating launch conditions are needed to determine the glass response and strength when mounted.
3. Correlate the analytical model to actual test data. This is particularly valid for determining two pieces of information, failure load and natural frequency. Any time a finite element model is developed, it is always necessary to ensure that the model is accurate to real-life data. If the model matches to the actual data, it ensures that the components used in the test are well understood (particularly the glass) and the model is an accurate representation of the baseline mirror-fixtured hardware.
4. Develop a baseline method for comparison of future mounting designs of the SXT mirrors. This test is the second of two tests performed on this mounting design. This test

seeks to develop a deeper understanding of the impact of an adhesive bond between thin D-263 glass shells and structural adhesive in a titanium groove. In the past year, numerous other promising mounting techniques have been identified, but all rely on a similar baseline design for the mirror-titanium structure interface.

## **CHAPTER 2: BACKGROUND**

### **2.1 Mission Overview**

The Constellation X mission is focused on discovering more details about a universe that is still not well understood. The primary mission of the Constellation X mission is to peer deep into the universe to perform X-ray spectroscopy on black holes, super novae and other astronomical phenomena. The estimated launch date of the mission is in 2017 by a Delta IV Heavy or an Atlas 5.

### **2.2 Science Goals**

In the past decade, recent astronomy discoveries have raised more questions than answers to our understanding of the universe. Modern telescopes such as the Hubble Space Telescope (HST), Keck Observatory in Hawaii, and Chandra X-ray Observatory have been able to only provide the first tantalizing steps to understand the context within our planet exists, not just in the galaxy, but the universe. It is within this context that the Constellation X-Ray Telescope is maturing as a part of NASA's "Beyond Einstein" program.

The Con-X telescope has a four fold goal. Constellation X attempts to answer vast questions like "What forces chiseled out the Milky Way, our neighboring galaxies and the billions of galaxies beyond the horizon? Where did the atoms in our body come from? What happens to space and time near a black hole? What is the fate of the Universe?" [7]. To help answer these questions, Constellation X focuses on black holes and the nature of gravity, dark matter and energy, and the formation of galaxies. As earlier researchers have discovered, the best way to study these subjects is by examining the X-ray wavelength of light. A brief description of each of these focus areas is discussed briefly below:

### *Black Holes:*

Recent science indicates there are three primary types of black holes, categorized by their size. Stellar black holes are typically the remains of massive stars that have exploded. The black holes at this level are believed to contain the mass of about 10-100 times of our sun. The intermediate black holes and super massive black holes are similar to stellar black holes, but contain even more mass (intermediate contains about 100-1,000 times more mass than our sun while a super massive black hole contains millions to billions more mass than our sun). Additionally, it is thought that most galaxies, including the Milky Way have a super massive black hole in the center. The gravitational pull of the spinning black hole is so strong that it bends or curves the fourth dimension, called space-time. Studying black holes can be difficult because their gravity is so strong that nothing can escape from the black hole, making it almost invisible. The black holes can be detected by their influence on the surroundings. One of these clues is the release of immense amount of energy from super heated gasses that are caught in the gravity of the black hole. The gas is heated from the friction due to the increasing speed of atoms and their resulting collisions [7]. This energy release is in the form of X-ray light and provides the best clues to the physics near black holes.

### *Life Cycle of the Universe:*

The second focus area of the Constellation X mission is to understand how elements are created and dispersed throughout the universe. Science has indicated this is predominantly accomplished through the explosions of stars at the end of their life, called supernovas. A supernova releases more energy than “our Sun does over 100 million years” [7]. The huge release of energy causes the “fusing” of mid-size elements such as carbon and iron into the heavier elements like gold and uranium. The elements created in this explosion, called the

supernova remnant, are then spread through the universe and “can be seen for tens of thousands of years”[7]. Using the X-ray spectra on the Constellation X telescope, scientist will be able to identify the quantity and types of elements created in these explosions.

#### *Galaxy Structure:*

Constellation X will enable scientist to see for the first time the motion of gasses within galaxy clusters. These measurements will be compared to current theories of cluster formation and evolution. The benefit of understanding how galaxy clusters are form and evolve is the first step to understanding basic processes throughout the universe.

#### *Dark Matter and Dark Energy:*

Recent discoveries in astronomy have led scientist to conclude that most of the mass in a galaxy is mass that we cannot see. In fact, it is estimated that “normal matter” makes up only 4% of the total Universe, while dark matter is approximately 25%, and the remaining 70% of universe is a mysterious force, discovered in 1998, that appears to be acting against the force of gravity and continues pushing or pulling the Universe farther out [7]. Constellation-X will be capable of providing the first tantalizing clues to understand these unique forces, called dark energy and dark matter, and role they play in the Universe.

### **2.3 Mission Design**

Constellation X will consist of four 1.6 meter diameter mirrors to study these science interest areas. The baseline design utilizes four identical formation flying telescopes to host each spectroscopy X-ray telescope (SXT) [8]. The Constellation X SXT will have the ability to detect light waves over a wider wavelength with a much higher sensitivity than previous telescopes. These two attributes, increased sensitivity and broader range of energy levels, is a major breakthrough for the ability of scientist to collect X-Ray data. It is estimated that Constellation

X will provide 10 to 100 times more data in the same time-span than is available from current operating telescopes [7].

The Constellation X telescopes will operate at L2, also known as the outer Lagrangian point. This location is unique because it uses the balance of the gravity from the Earth and the Sun to remain at constant position relative to the Earth and Sun. The outer Lagrangian point has several advantages for this mission. First, the orbit location prevents the Constellation X Observatories from entering Earth's shadow. Second, the temperature varies less at this location and the space environment is less influenced by Earth's proximity. Figure 2.1 presents a depiction to help the reader understand the positions between the Earth, Sun and Constellation-X orbit location.

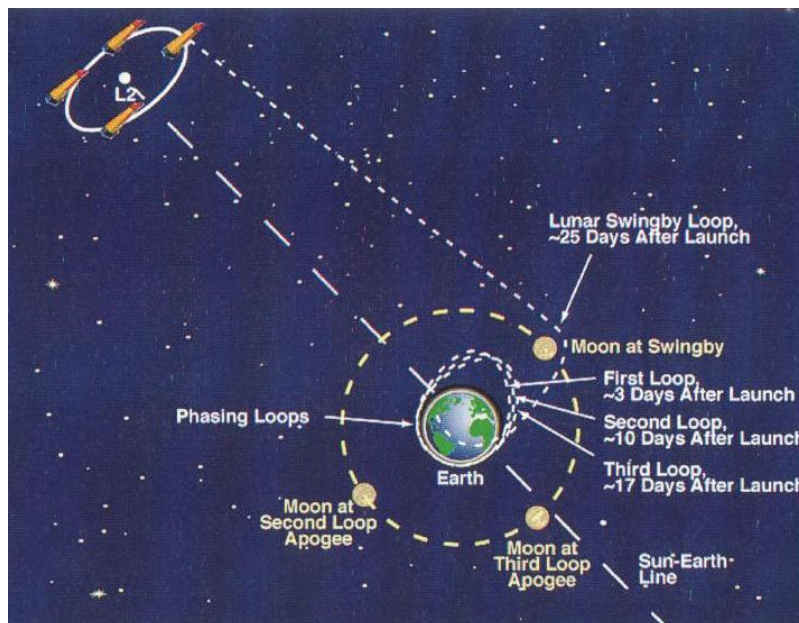


FIGURE 2.1: Positioning of Constellation X at L2 [9]

Constellation X will orbit nearly a million miles away from the Earth, which will preclude any astronaut missions to service the telescopes in the near future.

Before the Constellation X telescopes can reach L2, they first must be launched. It is currently envisioned that two telescopes will be launched at a time on either a Lockheed Martin Atlas V or a Boeing IV Heavy. As a result it will take two launches to put the full Constellation X into orbit. While this does increase the cost of the mission by paying for two launch vehicles, it also prevents a catastrophic failure during launch or maneuvers to orbit from causing a complete failure of the Constellation X mission. Figure 2.2 presents a possible configuration where two telescopes could be nested inside the Delta IV fairing for launch. Several burns will be required once the telescopes are orbiting Earth to position them at the appropriate location at L2.

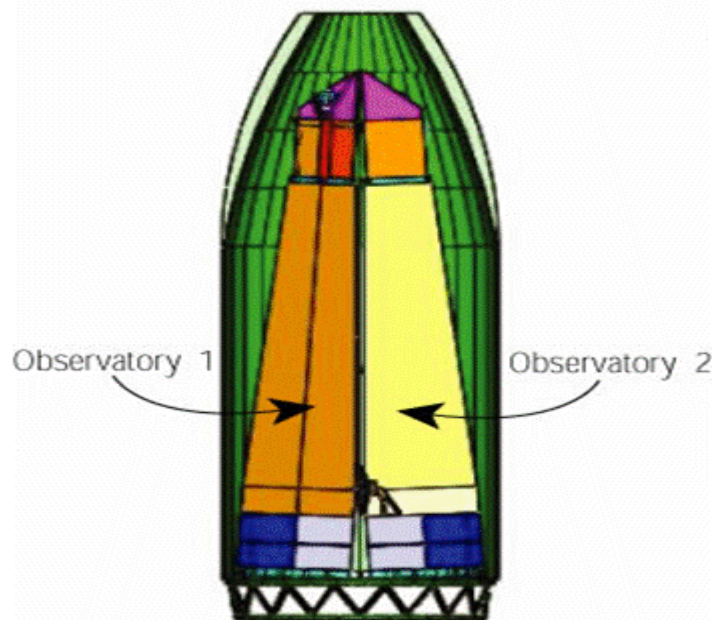


FIGURE 2.2: Constellation X Launch Configuration for 2 Observatories [8]

## 2.4 Constellation X Telescope Design

As previously discussed, the Constellation X mission will rely on up to four identical spacecraft to perform the mission. Each spacecraft will carry one spectroscopy X-ray telescope

(SXT), or called “soft X-ray.” In addition, each spacecraft will have three hard X-ray telescopes capable of making observations from 6 keV to 40 keV. This will ensure an ability to provide continual observations across majority of the X-ray energy band. A possible spacecraft design is shown below in Figure 2.3:

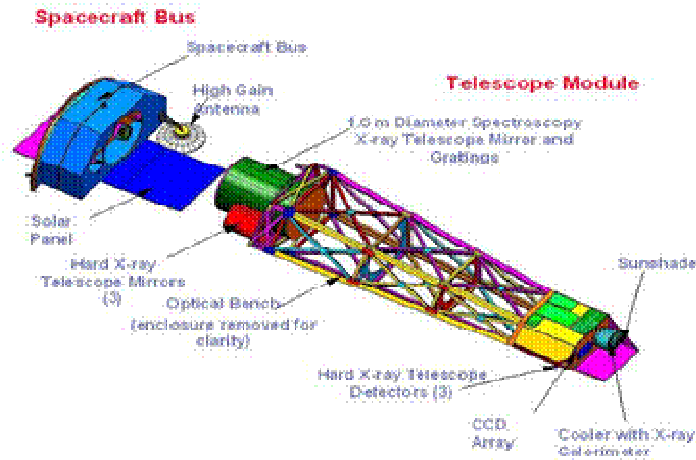


FIGURE 2.3: Constellation X Baseline Design [8]

As annotated on the figure, there are several other critical components necessary for the SXT to achieve success for the Constellation X mission. Figure 2.4 below shows the path of the collected X-Rays to the detection devices. After the X-rays are reflected through the SXT by grazing incidence, half of the converging X-rays pass through reflective gratings to the CCD. The remaining half of the convergent X-ray beam is collected by the calorimeter. The CCD and calorimeter enable the SXT to perform the necessary spectroscopy analysis to perform the mission. The current requirements for the SXT mirrors are shown below in TABLE 2.1.

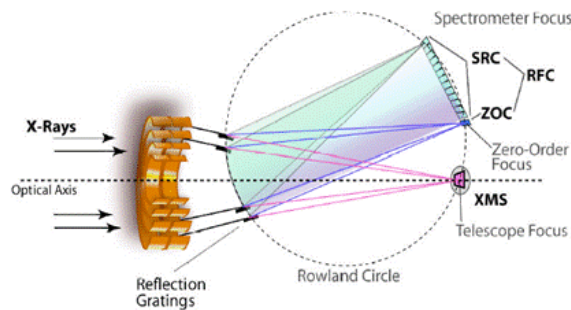


FIGURE 2.4: X-Ray Reflection Path and Detection Devices [9]

TABLE 2.1: SXT Mirror Requirements [10]

Parameter	Value
Axial distance from the primary-secondary intersection plane to telescope focus	10,000 mm
Primary and secondary mirror axial lengths	200mm – 300mm
Maximum reflector radius at the intersection plane	800 mm
Minimum reflector radius at the intersection plane	~150 mm
Axial distance from the back of the primary to the intersection plane	25.1 mm
Axial distance from the intersection plane to the front of the secondary	24.9 mm
Gap between the primary and secondary	50 mm
Mirror shell thickness	0.44 mm
Telescope field of view	2.5x 2.5 arc-minutes
Total mass per SXT (including 75 kgm for reflection grating assembly)	750 kgm
Mechanical Envelope	1700 mm D x 2060 mm L

Initial engineering analysis performed by the Constellation X team has formulated a baseline design. It is important to note that many of these characteristics could (and most likely will) change as the design evolves in the coming years. Currently, the SXT is envisioned to have a 1.6 m diameter mirror built up of nested arc segments using slumped Schott D-263 glass with a reflective gold coating.

The SXT uses a Wolter Type I grazing incidence mirror to collect the low power X-rays. Using a Wolter Type I telescope design allows larger diameter mirrors to be used that are otherwise too heavy for space observatories using a traditional design. The Wolter Type I design relies on two sets of concentric circles of mirrors to reflect the X-rays using grazing incidences. The upper concentric circles of mirrors are formed in a parabolic shape (primary mirrors), while the lower concentric circles follow a hyperbolic shape (secondary mirrors). There are between 170-230 mirror shells of varying radii for the primary and secondary mirrors. The smaller radii shells are housed in the six inner modules and have a 60 deg arc segment. The outer radii shells are located within 30 degree modules (a total of 12) with a corresponding 30 deg arc segments. The SXT structure is shown in Figure 2.6.

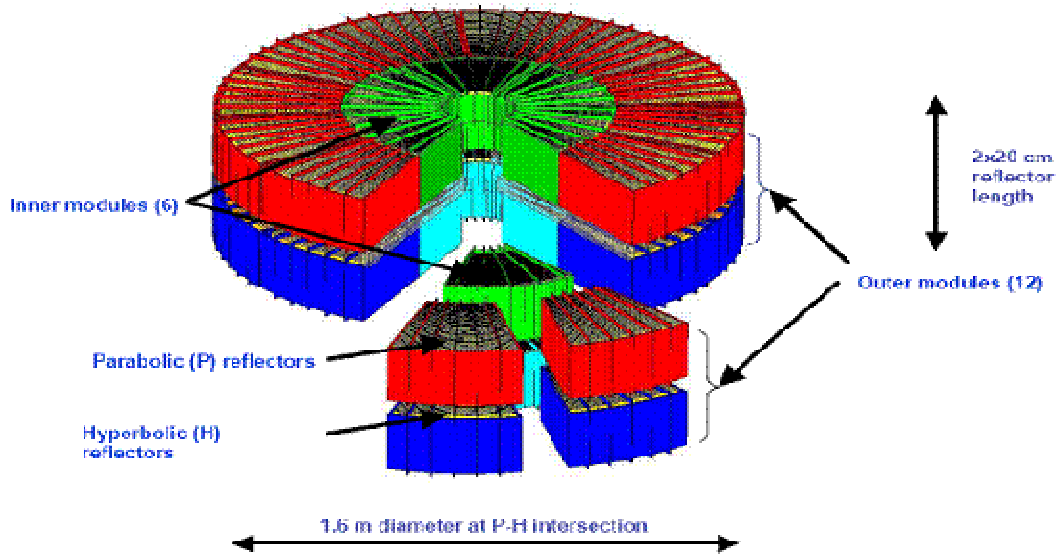


FIGURE 2.5: SXT Mirror Buildup [8]

Figure 2.6 also shows the modules that are used to hold each of the mirrors. The mirrors are 0.4 mm thick and varying in height from 20 to 30 cm. Based on this design, there are somewhere between 3012-4140 mirrors in each SXT assembly.

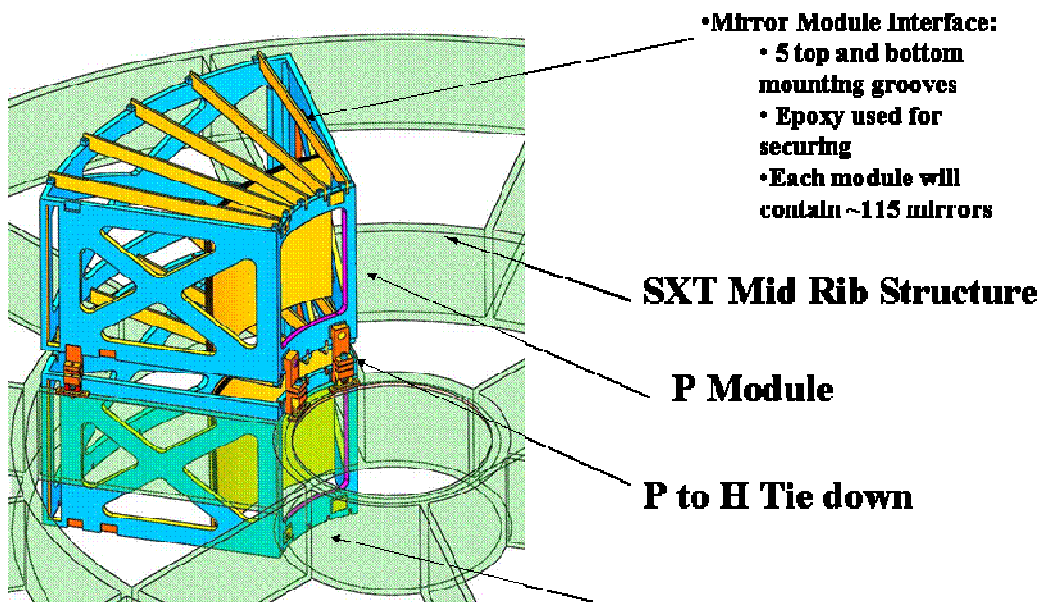


FIGURE 2.6: SXT Mirror Housing [12]

The SXT requires an overall accuracy of 15 arc seconds for the combine optics to achieve the desired resolution. Each and every of the 3,000 mirror segments in one SXT must be positioned within 0.5 microns to meet this requirement. As a result, methods used in the past for optical alignment of mirrors must be modified or completely thrown away to achieve the required placement accuracy in a timely fashion of at least 12,000 mirror segments.

To investigate possible methods and some of the unknown issues when attempting to place and hold mirror shells at such precise tolerances, a development plan was created to “build-up” to the necessary level of precision. Previous work identified a ten point mount (five points on top and five on bottom of the mirror segment) as the most effective way to hold each mirror shell [13]. The first attempt to align a pair (one primary and one secondary) mirror was called OAP 1, shorthand for Optical Assembly Pathfinder 1.

## **2.5 Optical Assembly Pathfinders**

The goal of the OAP is to evaluate the most effective way to manipulate the positioning of a mirror segment when positioned in the housing module using five top and bottom points. Several other requirements were established for the initial OAP shown in Figure 2.7. This includes [12]:

- Accommodate one Primary and Secondary optic 20 cm in length with radii near 25 cm
- Represent an inner module
- Be made of Aluminum
- Facilitate optic alignment by the CDA
- Facilitate the determination of a single optic alignment process
- Facilitate the creation of a plan to establish the optic absolute radius

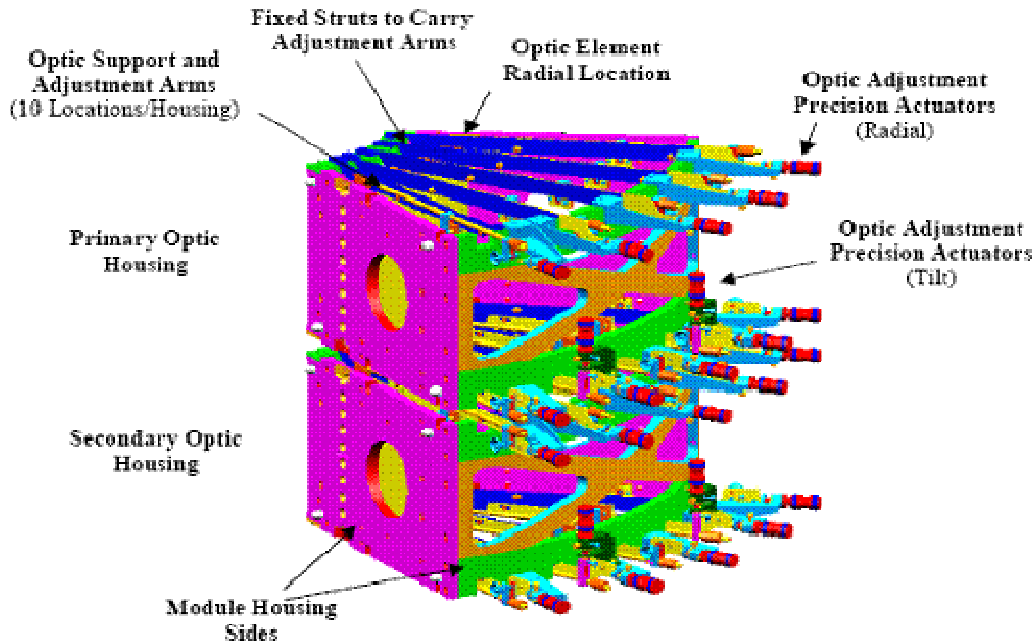


FIGURE 2.7: Optical Assembly Pathfinder 1 [12]

The OAP 1 design shown in Figure 2.7 is based on an inner module from the SXT and positions one primary and secondary mirror. The module structure was machined out of aluminum to decrease cost and time to build the initial OAP design. Future OAP designs rely on a titanium alloy that more closely matches the coefficient of thermal expansion value (CTE) for the D-263 glass and has higher strength to weight ratio. The adjustments on the top and bottom are hand activated using precision actuators along with an 11<sup>th</sup> actuator used to adjust the tilt of the mirrors. This initial OAP1 design was primarily used to learn how to insert and remove mirrors from the housing module and evaluate the effectiveness of adjusting mirror shell positions via radial adjustments. A more complete analysis of the lessons learned can be found in the paper by Scott Owens, et al.

After the successful the work accomplished on OAP1, OAP2 was manufactured. The need for OAP2 grew out of the successful manufacturing of mirror substrates that required the ability to perform a “quick” X-ray test. The OAP2 design is unique because it builds on and uses

OAP1. OAP2 module is designed to fit within OAP1 and uses OAP1 precision actuators. The module is designed as a single monolithic titanium structure. Titanium was used in this module to reduce CTE mismatch between the structure and the mirror since this module would undergo optical evaluation. Please note in that the structure has no moving parts and is comprised of titanium.

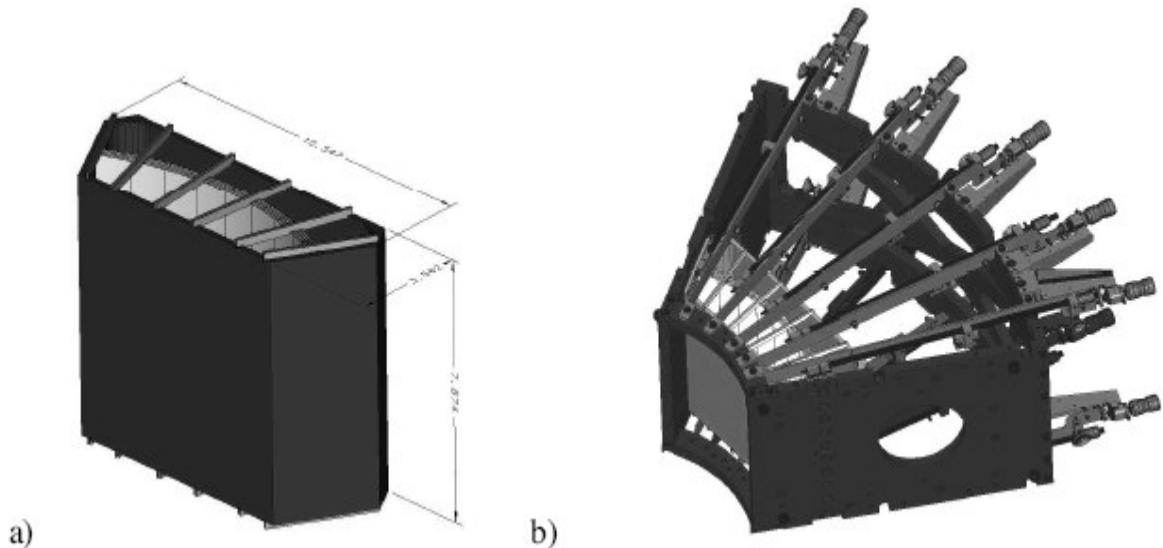


FIGURE 2.8: a) Optical Assembly Pathfinder 2 b) OAP2 nested within OAP1 [14]

As previously stated, OAP2 “sits” inside of the OAP1 housing during alignment. The OAP2 mirror segments are positioned using the same method as was used for OAP1. After the alignment is complete using the 11 precision adjustors (10 radial position and 1 tilt), the mirror segment is bonded to the titanium struts of the OAP2 housing. [14] Grooves are cut at the approximate location on each titanium strut, while the epoxy is used as a liquid shem to maintain the mirrors position as closely as possible once the OAP2 module is removed the precision adjustors and the OAP1 housing. Initial plans called for the OAP2 housing to be subjected to vibration testing after completion of X-ray tests. Due to funding constraints, the vibration test was modified and reduced. The new vibration test is the subject of this paper.

## 2.6 Glass Properties

All mirrors for the Constellation X SXT telescope use thermally slumped Schott Desag 263 glass. This material was selected after an extensive examination of available materials based on optical and slumping properties. This is a mixed alkali glass similar to pyrex and has several advantageous characteristics including a low coefficient of thermal expansion (CTE), high resistance to chemical attack, and low slumping temperature.

Properties of glass are unique when compared to materials. Even a definition of what is a glass is difficult to ascertain. According Arun Varshneya's Fundamentals of Inorganic Glasses, glass is commonly defined as an “amorphous solid that undergoes a ‘glass transition’ when heated,” where glass transition is defined as a “continuity of volume and a steep change in physical properties such as specific heat, thermal expansion, etc” [4]. Figure 2.7 is a volume-temperature diagram for a glass forming liquid which highlights the unique transition area of glass.

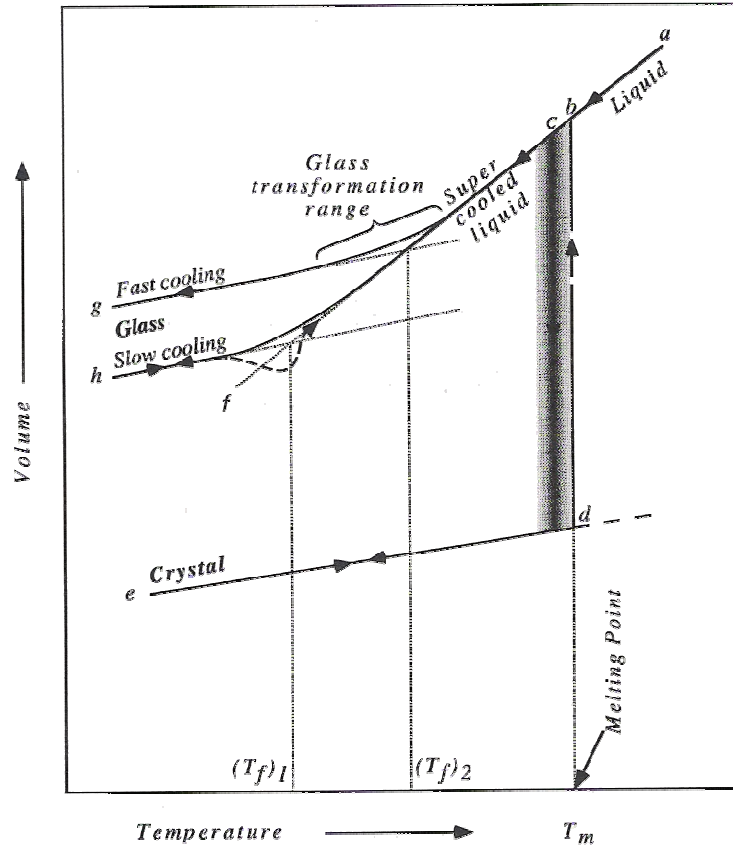


FIGURE 2.9: Volume-Temperature Plot for Glass Forming Material [4]

To understand Figure 2.9, consider an amount of glass forming material at high temperature in liquid form. This state is given at point *a*. As this liquid is cooled, the temperature and volume relation moves along the *a-b* curve. At point *b*, the temperature of the liquid is at the melting point of the corresponding crystal,  $T_m$ .  $T_m$  signifies an “infinitely small amount of crystals is in thermodynamic equilibrium with the liquid”[4]. In order for there to be a noticeable level of crystallization, the temperature must be further decreased to some lower point, this is denoted as point *c*. This region of crystallization is shaded to indicate the varying possibility of the crystallization path along with a volume decrease. After further cooling, the crystals move along path *d-e* to *e* with the accompanying volume decrease. If the cooling rate sufficiently high, the *liquid* material will move along the *super cooled liquid (bcf)* line that is

extrapolated from the *abc* line. The volume of the material continues to shrink due to restructuring of the molecules to match the lower energy due to the decreased temperature. This cooling causes the molecules to rapidly loss mobility. Eventually, the molecules no longer have the ability to rearrange themselves to correspond to the lower energy levels, resulting in a higher volume than seen at the crystal state. The volume temperature line extrapolated from the path *abf* then begins to diverge from the actual properties of the glass. The volume-temperature of the glass curves from the extrapolated path and becomes a near straight line ending at point *g* if cooled at a high rate, or *h* when cooled at a lower rate. The resulting straight line is usually parallel to the line *ed*, and represents the glassy state of the material.

The curve shown where the volume temperature path departs from the super cooled liquid path and becomes linear, represents the glass transition range. The glass transformation range is usually ranged by viscosity levels where the upper regions has a viscosity of  $10^9$  poise and the lower region is typically around  $10^{14}$  poise or more to “qualify for appearance as a solid”[4]. The fictive temperature represents the temperature level at which the atomic structure of the super-cooled liquid is instantaneously frozen. It is important to note that lower cooling rates will typically produce glass at greater densities than at higher cooling rates. However, the densities of the glass will be less than the corresponding crystal. The cooling rates must be controlled while within the transition region to ensure properly slumped glass.

Besides the affect of the cooling rates on glass structure, Varshneya highlights two unique properties of glass that make it difficult to determine a single number for the “strength” of glass, as is typical for metals:

- (i) “Most metals neck or yield plastically before actual failure occurs whereas glasses do not show any ductility prior to the failure. We say that the metals show ductile failure and the glasses show brittle failure.”
- (ii) “Whereas a given group of metal specimens prepared identically shows a narrow distribution of yield stress and ultimate fracture stress, glass specimens produced apparently identically are likely to display a large variation of strength.”

The crystalline structures in metal allow “dislocation defects” to be shifted according to applied stresses to a certain point. Glasses have no or little ability (in special circumstances) to shift those dislocation defects. This lack of ability is easily seen in the brittle behavior of the material. This brittle behavior also plays a part in the wide variation seen in the strength of identical glass samples. The flaws in glass are unique because it actually results in the creation of two new surfaces, where as in metals, the dislocation can shift without breaking the atomic bonds. This results in a wide variation of strength measurements based on specimen size, surface condition, and environments [4].

Due to the unique nature of glass strength, failure analysis of glass requires the use of the weakest-link criterion. According to the weakest-link criterion, “the body will fail when the stress at any defect is sufficient to cause unstable crack propagation of that defect” [4]. There are several weakest-link criterion probability density functions including the Weibull distribution, flaw density distributions, and extreme-value distributions. According to Varshneya, “the Weibull distribution is the most popular because of its mathematical simplicity and closer agreement with experimental data.” The equations for the Weibull cumulative probability of failure (P) are given below in equation set 1 and 2.

$$P = 1 - \exp[-R] \quad (1)$$

The variable  $R$  denotes the risk of rupture and is given by the following equations:

$$R = \int_V [(\sigma - \sigma_u) / \sigma_o]^m dV \quad (\text{for } \sigma > \sigma_u)$$

$$R = 0 \quad (\text{for } \sigma < \sigma_u) \quad (2)$$

Where  $V$  is the volume,  $\sigma$  is the stress over a finite volume ( $dV$ ),  $\sigma_u$  is the minimum stress for failure,  $\sigma_o$  is a normalizing stress parameter.  $M$ , Weibull modulus, along with  $\sigma_o$ , are typically calculated from empirical data using statistic analysis software. The lower the value of the Weibull modulus, the more spread in the data. The cumulative probability function ( $P$ ) and the probability density function ( $p$ ) can be rewritten to include volume and loading constraints in a simplified version as follows:

$$P = 1 - \exp\left\{-\left[\sigma / \sigma_o\right]^m\right\} \quad (3)$$

$$p = dP / d\sigma = [m / \sigma_o] \left[\sigma / \sigma_o\right]^{m-1} \exp\left[-\left(\sigma / \sigma_o\right)^m\right] \quad (4)$$

The strength test performed at NASA used the Weibull distribution to develop an understanding of the strength of D-263 glass. While it is apparent that glass samples with varying defect distribution will produce varied strength values when tested in similar fashions, the converse is also true, glass samples with identical flaw distributions are likely to produce varying “strength distributions when tested in varying modes” [4]. As a result of this known behavior, the Constellation X team pursued, in addition to glass sample strength testing using ring-on-ring and bending tests, vibration tests with the mirror mounted in configuration similar to the current flight design.

## 2.7 Schott Desag 263 Glass Properties

Prior to the strength tests performed by the Constellation X, little information was available concerning Schott Desag 263 glass. There was even less information on the strength of thin sheets (on the order of 0.4 mm) after slumping. Table 2 presents the published Schott D-263 glass properties.

Table 2.2: Schott Desag 263 Glass Properties [15]

<b>Viscosity and Corresponding Temperature</b>		
Designation	Viscosity	Temperature
	$\log \eta$ [dPas]	$\theta$ [°C]
Strain Point	14.5	529
Annealing Point	13	557
Softening Point	7.6	736
Transformation Temperature $T_g$ in °C		557
<b>Coefficient of Thermal Expansion <math>\alpha</math></b>		
Coefficient of Mean Linear Thermal Expansion $\alpha_{(20-300^\circ\text{C})}$ in $10^{-6} \text{ K}^{-1}$ (Static Measurement)		7.2
<b>Mechanical Properties</b>		
Density $\rho$ in $\text{g/cm}^3$ (annealed at $40^\circ\text{C/h}$ )		2.51
Stress Optical Coefficient C in $1.02 \cdot 10^{-12} \text{ m}^2/\text{N}$		3.4
Young's Modulus E in $\text{kN/mm}^2$		72.9
Poisson's Ratio $\mu$		0.208
Torsion Modulus G in $\text{kN/mm}^2$		30.1
Knoop Hardness $\text{HK}_{100}$		590

Since glass strength is difficult to determine, NASA GSFC initiated a series of strength test designed to develop a greater understanding of D-263 glass strength and mechanical properties. The series of test also looked how manufacturing processes such as cleaning and slumping affected the glass strength.

## **2.8 Constellation X SXT Slumping Process**

The manufacturing process of the glass substrates has undergone constant change at NASA Goddard. It is a multi-step process, requiring precise controls at each point to ensure that the glass meets the stringent requirements of Constellation X. This process includes not only slumping the glass into the proper shape, but also cutting the slumped glass and depositing thin layer of gold on the surface of the glass substrate to enhance reflective qualities.

The glass arrives from Schott Glass in 400 micron glass sheets. The glass sheet is then laid on a fused quartz mandrel and placed inside an oven. Over the next several hours, the temperature is raised to 570 F, the glass is held at this temperature for several hours, before a gradual ramping down of the temperature. Recent work has been focusing on the reduction of internal stresses due to uneven cooling rates that affects the mirror shape. After the slumping process is completed, the glass substrate is cut by a nickel chromium hot wire to the proper dimensions. The substrate is then placed on another mandrel, called the replication mandrel. This mandrel is used to deposit a thin layer of gold on to the substrate. Previous work required that the glass substrate be sprayed with a thin layer of epoxy before placement on the replication mandrel, however the lead scientist in this area at NASA Goddard, Dr William Zhang, has developed a process where no epoxy is required. By removing the layer of epoxy, it removes another variable that could reduce the optical quality of the mirrors.

The gold coating is the last step before the mirror can be measured for optical or strength qualities. While the process appears straight forward, there have been numerous difficulties that have only recently been overcome. The substrate manufacturing process is well matured and recent efforts have focused on evaluating glass strength and optical properties after processing.

## 2.9 Strength Testing

The strength testing of D-263 glass was performed through five stages. All work was performed at NASA Goddard. Testing used a biaxial test technique on (sometimes called ring-on ring) flat glass samples shown in Figure 2.10.

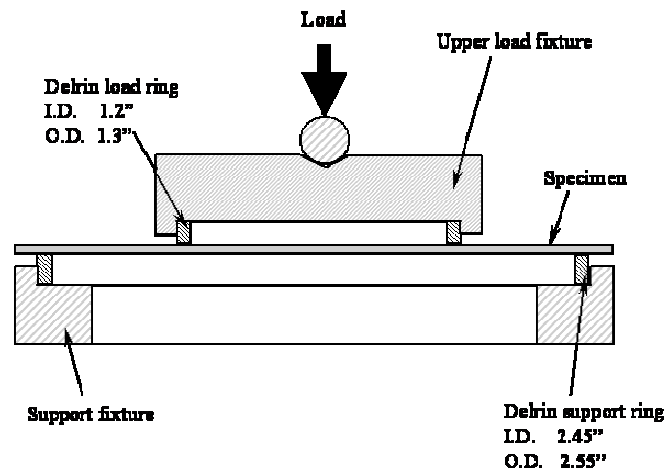


FIGURE 2.10: Biaxial Strength Testing Setup [16]

These tests included slumped and non-slumped glass pieces in three inch flat squares. It is important to note a few things about this type of test. First, ring-on-ring test primarily examines surface defects while edge defects are not evaluated in this type of testing. This is consistent with expectations since the load is applied completely on the surface of the glass via a loading ring. After the completion of each test, the data is used in a finite element model (FEM) to determine the strength of the sample. All of the glass samples have thickness on the order of 0.4 mm. This is significant because the deflection from the load is much greater than the thickness of the glass. Non-linear effects must be taken into account in the FEM since deflections are greater than the glass thickness. FEM model looks at only one quadrant of the glass stresses because the ring is assumed to be perfectly centered on the glass piece as shown in Figure 2.11. As a result, the strength calculations for the remaining three quadrants will produce the same load distribution.

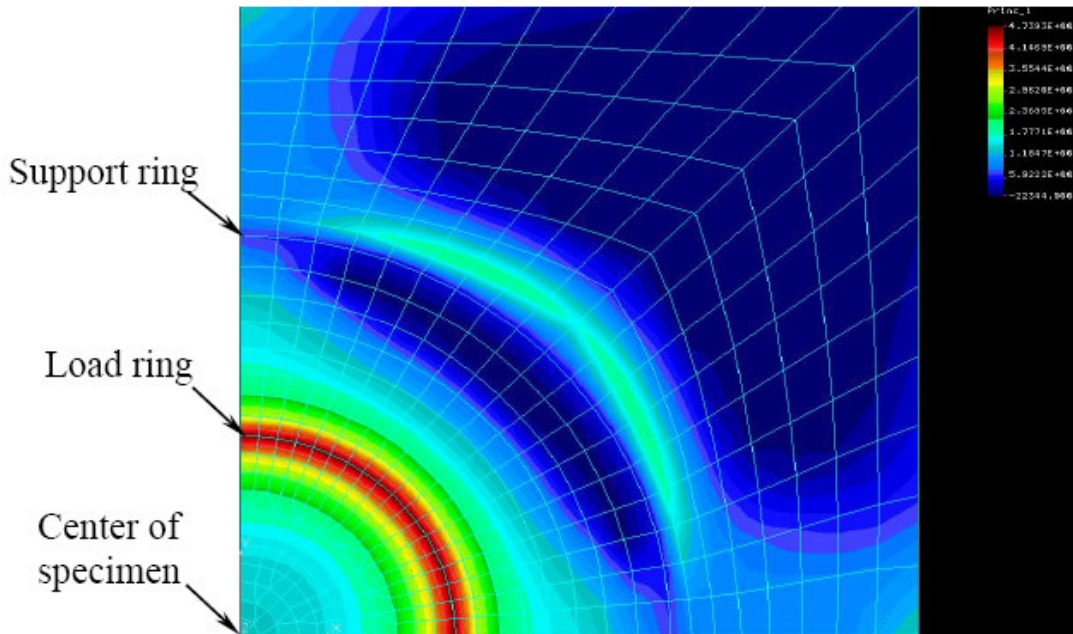


FIGURE 2.11: FEA Model for Biaxial Strength Testing for 1 Quadrant [16]

A second type of test used for evaluating mechanical properties of glass shells. The bending test used for the glass shells is shown in Figure 2.12. The mirror is placed between two loading blocks. Because glass fails when in tension, kapton tape is added to the compression side of the mirror to help reconstruct the failure point of each sample. Additionally, since the load is placed on the edge of the sample, edge defects are examined during this testing. A FEM is used to analysis the strength of the shell after failure in a process similar to that used on the flat square samples using the nonlinear solution. The location of maximum stress is shown in Figure 2.13 at the along the “spine” of the curve. The area of high stress is denoted in red.

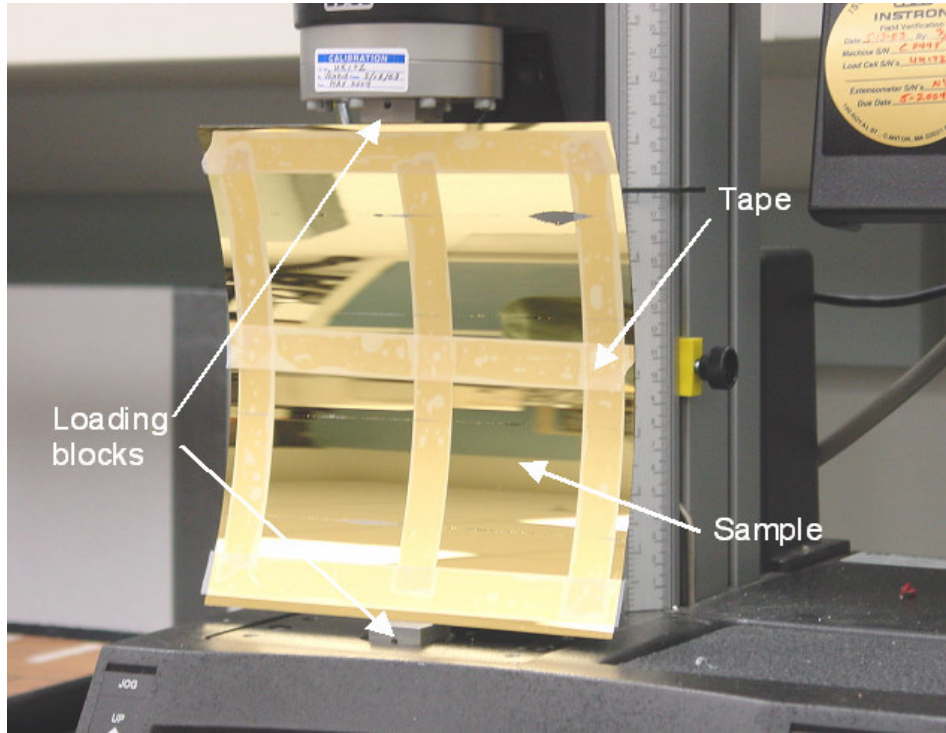


FIGURE 2.12: Bending Strength Testing Setup [6]

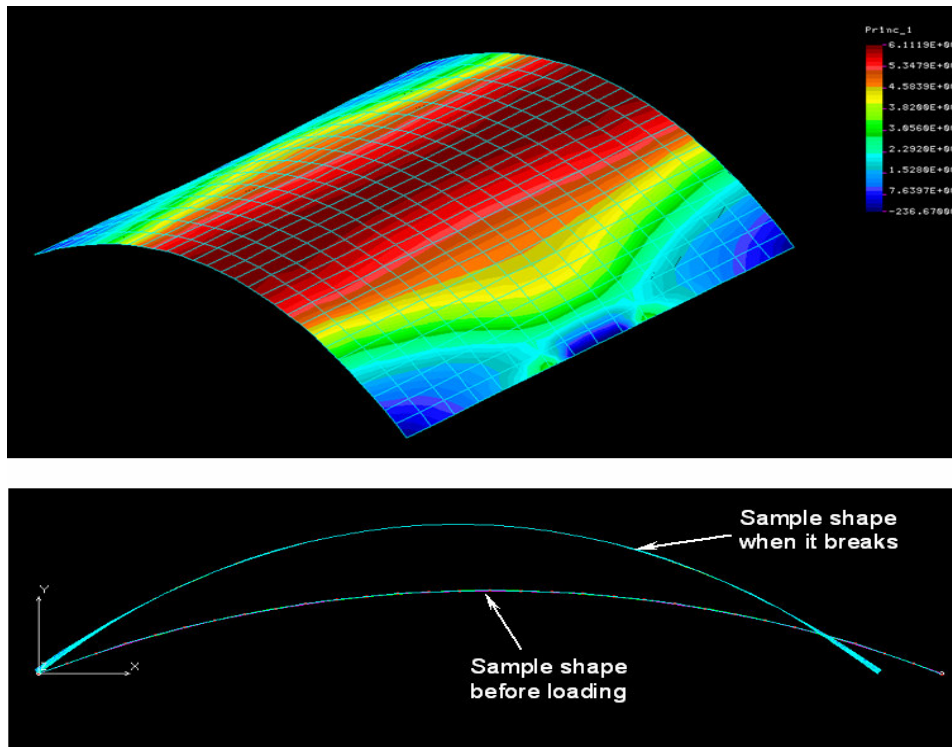


FIGURE 2.13: FEA Results for Bending Tests [23]

### 2.9.1 Strength Test Results from 1999 Biaxial Test

Testing started in 1999 in cooperation with the Smithsonian Astrophysical Observatory (SAO) and examined a range of materials with varying sizes and thicknesses. Two types of glass supplied by Schott were tested, D-263 of thickness 0.3 mm and 0.9 mm, and AF-45 of 0.3 mm and 1.1 mm thickness. Additionally, silicon wafers were evaluated in the same range of thickness. The major result of these tests was the determination that the slumping of the glass results in almost a 50% reduction of the glass strength. It is important to note that all of these tests were ring-on-ring tests which considered only surface defects.

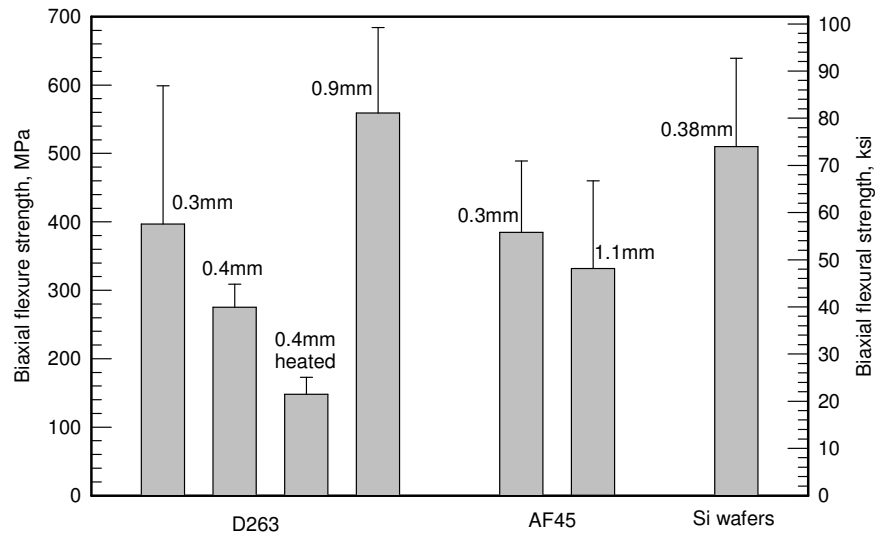


FIGURE 2.14: Results from 1999 Strength Tests [16]

### 2.9.2 Strength Test Results from 2003 Bending Test

Earlier tests highlighted a need to perform further evaluations to understand the characteristics of D-263 glass after receiving a coating a reflective coating. In late 2003, a series of tests were undertaken to understand the effect of the gold and silver coating on slumped D-263 glass shells. 12 shells were tested, 7 coated with approximately 20  $\mu\text{m}$  of epoxy and gold, 2 coated with silver, and 3 without any coating. The thickness of the glass was on the order of 400

μm. As with all of the glass shell strength tests, a bending test is utilized where the load is applied at the edge of each glass shell. If the mirror has no surface or edge defects, the sample should break straight across the “fold” of the piece. The resulting load-displacement curves are shown in Figure 2.15.

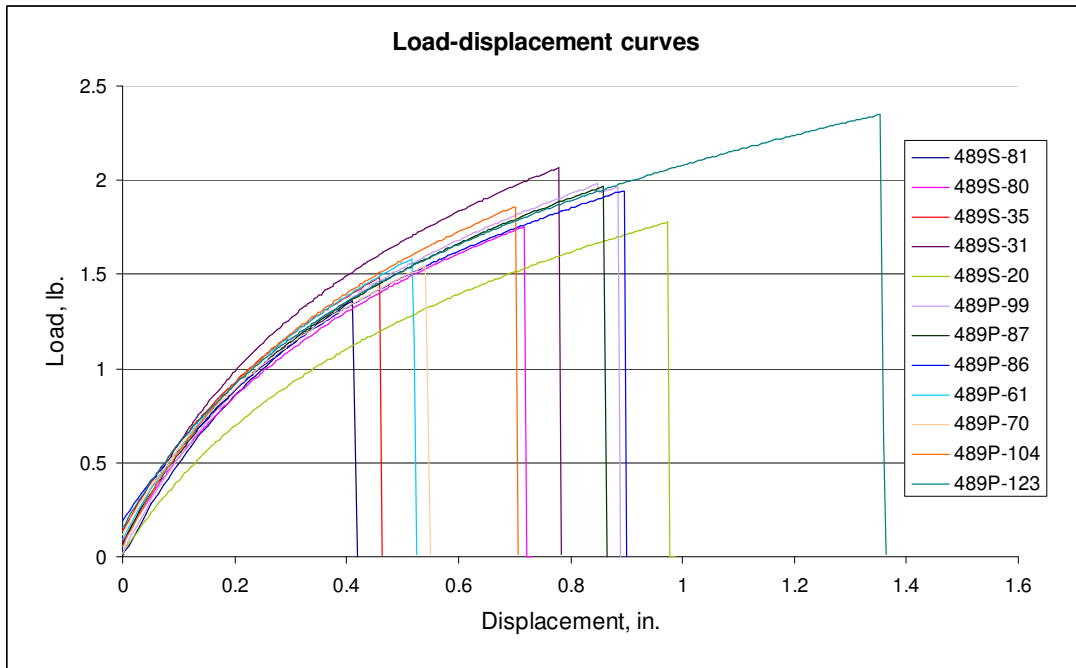


FIGURE 2.15: Load Displacement Curves for Glass Shell Strength Tests [16]

Again, these are used in a FEA model to determine the actual failure strength of each sample and an example can be seen in Figure 2.13. Note the higher stress loads along the center of the mirror and the stress concentrations at the loading locations. The results for the clear glass and gold-epoxy coating are fairly consistent while the two silver coating appear at a lower strength but still within the uncertainty of the strength samples as seen in Figure 2.16.

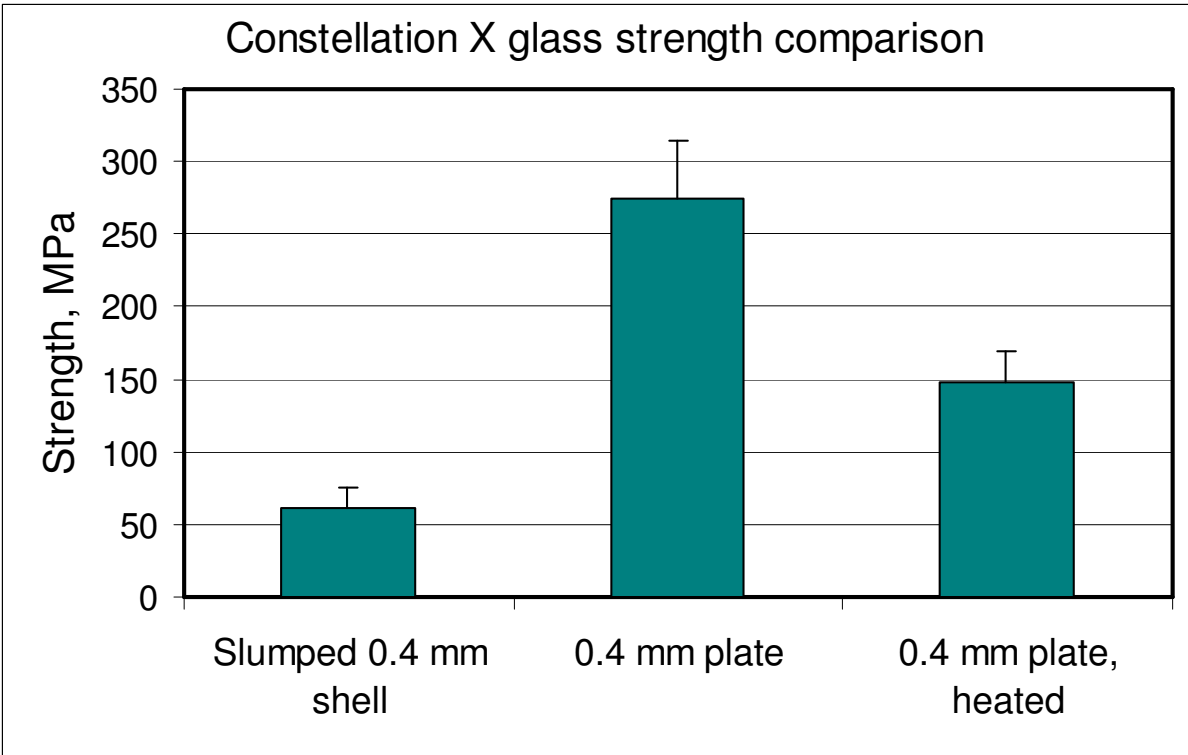


FIGURE 2.16: Constellation X Slumped Shell Strength Comparison [16]

To gain an understanding of the effect of slumping the flat glass pieces into “curved” pieces, the strength results are plotted against previous flat sample tests. As is evident from the plot, slumping the glass in to curved a shape significantly reduces the strength. The strength of the slumped glass shells is 61 MPa (8.7 ksi) with a range of 13.9 MPa (2.0 ksi) Nearly 50% of the samples failed due to edge defects, while the remaining samples failed due to surface defects.

### 2.9.3 Strength Test Results from 2004 Biaxial Tests

The next step to understand D-263 glass was to identify the critical strength issues. The two areas identified by the Constellation X team are the differences between glass batches supplied by Schott glass and the effects of the cleaning the glass. By identifying the affects of each of these variables on the glass strength, it may be possible to isolate issues that can cause a severe reduction in glass strength. The batch strength evaluation is performed over a set of four

different deliveries. Each “delivery” consists of one 11.5” x 14” plate that is cut by diamond scribe to 20 samples of approximately 3.5” squares.

To evaluate the effects on cleaning of the glass plates, five plates were cleaned using the same procedures as for the slumped shells and then cut to 3.5” squares, resulting in about 15 samples. Testing in both areas used the ring-on-ring strength test method and a one quadrant FEA model to determine stresses. Kapton tape was also used in both tests to determine fracture origin and pattern.

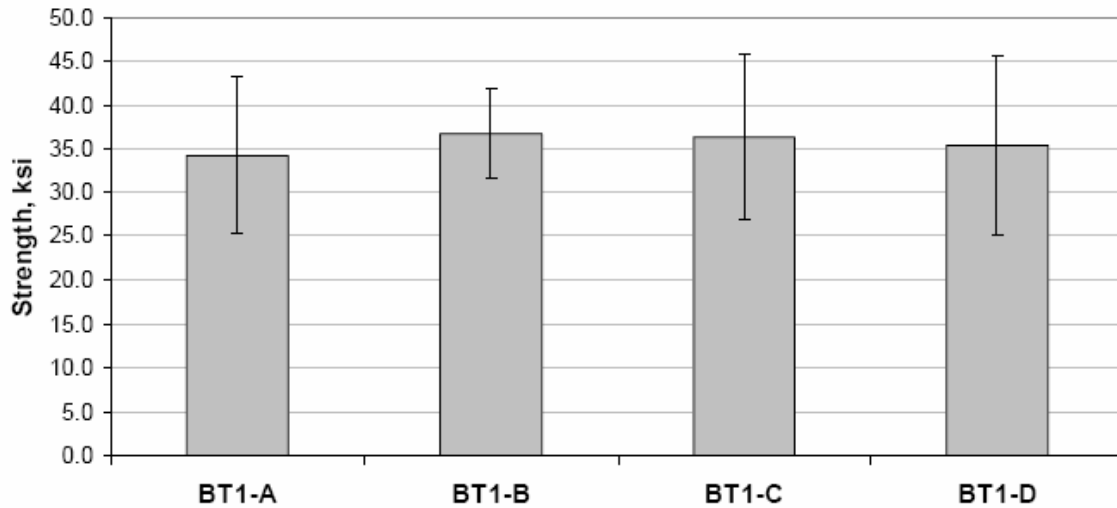


FIGURE 2.17: Strength Comparison of Four Schott D-263 Glass Deliveries [16]

Figure 2.17 shows the resulting strength variation among deliveries. It is easily discernable that the strength of the different deliveries is within the standard deviations. This indicates strength differences are not significant. All deliveries have similar average strength, but A, C, and D deliveries shows a much larger amount of scatter among the data. Interestingly, delivery B has the same average strength, but substantially less scatter, resulting in a higher Weibull modulus.

The knowledge gained from comparing strength of varying deliveries was then applied to evaluate the effects of cleaning on the glass. For the comparison, the glass sample data from the delivery comparison, denoted by the BT1, was used as the baseline to compare an addition 53 cleaned samples. Figure 2.18 presents the result of this test. The average strength of the BT1 samples was found to be 246 MPa while the cleaned samples (BT2) were found to have a strength of 224 MPa. Further statistical analysis found the difference was statistically significant at the 90% confidence level [16]. BT2 data, besides 9% lower average strength, showed significant scatter. This is consistent with expectations because the cleaning process is hand done and may vary with each sample.



Figure 2.18: Glass Strength Comparison between Deliveries and Cleaning [16]

#### 2.9.4 Strength Test Results from 2005 Biaxial Tests

The 2005 work focused on further quantifying the effects of slumping D-263 glass. Earlier tests had indicated that the slumped glass strength is significantly reduced but insufficient samples were used to perform a more in-depth statistical analysis. In this investigation, 20 glass plates (3.5" x 3.5") were slumped flat and evaluated using the ring-on-ring strength testing that was performed on BT1 (variability among glass deliveries) and BT2 (cleaning effects). Many of

the same preparatory and evaluation processes were used in this testing as before such as finite element modeling using the non-linear elastic modeling and Kapton Tape to identify failure location.

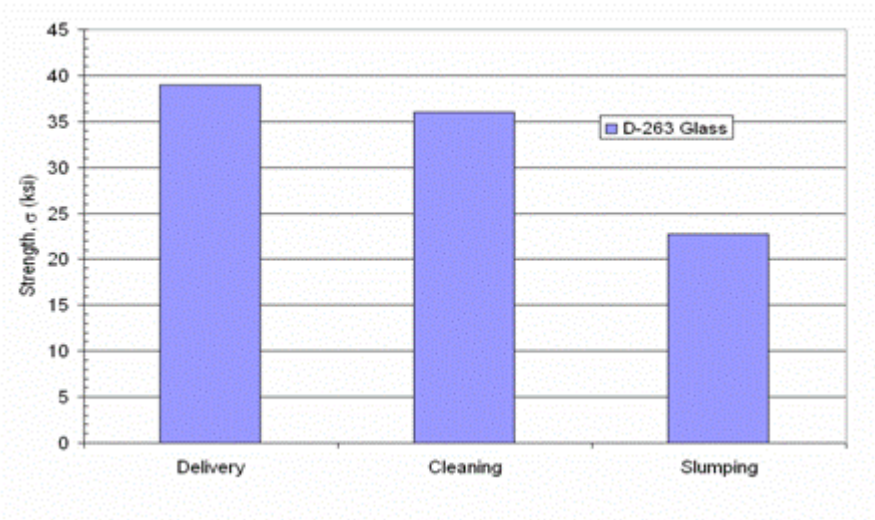


FIGURE 2.19: D-263 Strength Comparisons [16]

After slumping the glass samples, the average strength was found to significantly decrease. Figure 2.19 presents the culmination of the data found on the average strength of D-263 glass samples including 156 MPa for the average strength of slumped samples. 11 of the 20 samples failed due to “surface dimples” [16]. The dimples were likely caused by glass contamination while on the mandrel or during the slumping process. A scanning electron microscope (SEM) was used to observe the dimples, an example of a typical dimple is presented in Figure 2.20.

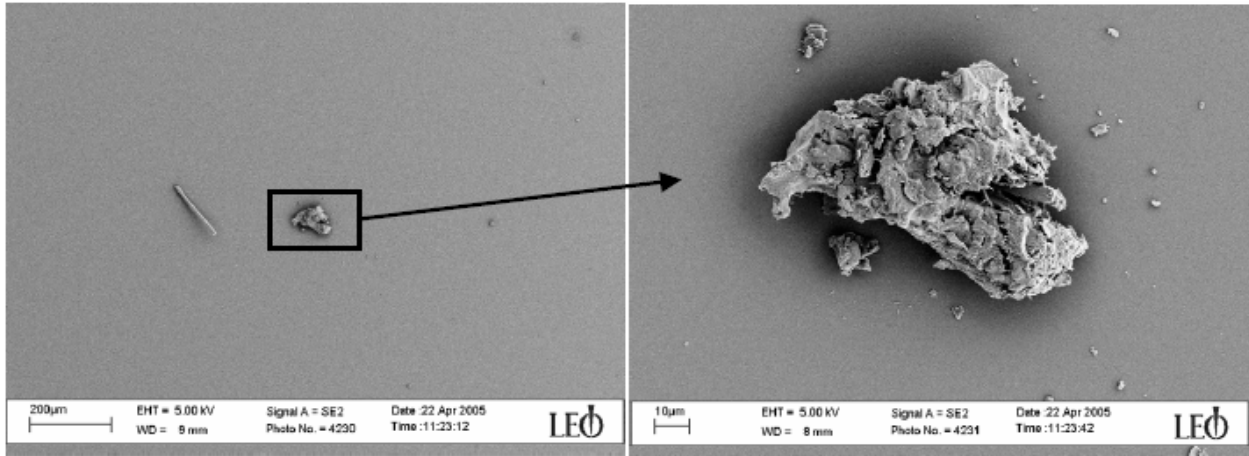


FIGURE 2.20: Typical Particle Contamination found in D-263 Glass [22]

### 2.9.5 Strength Test Results from Chemically Strengthened Glass

During the early strength testing stages of the glass, the Constellation X team also investigated methods to increase the strength of D-263 glass. At the basic level, chemical strengthening relies on an ion exchange process where small ions are exchanged for larger ions through diffusion by immersing the glass in a molten salt bath. This creates a very thin surface layer where the glass is held in compression because of the increased size of the ions. This process of “ion exchange” was first introduced in 1962 by Kistler, Acloque, Tochon, and Sendt [17]. The mechanical engineering members of the Constellation X team paired up with Dr Arun Varshneya at Alfred University and Saxon Glass to determine the feasibility of strengthening this glass. The ion exchange method was selected because of the numerous advantages over other strengthening processes such as thermal tempering when compared to the requirements for the SXT telescope. Major advantages include the ability to double or triple the strength of the glass and retain the slumped shape of the glass [17]. Since glass typically fails in tension due to crack growth beyond the sub-critical size, the compression layer substantially delays the crack growth. The glass shape can be retained because the temperature is held below the glass transition

temperature while in the molten bath. Testing for the Constellation X team has primarily focused on evaluating the strength enhancements resulting from this chemical treatment.

Several months were required at the beginning of the investigation to determine the best way to control the process for D-263 glass. The exchange process for each piece of glass can last anywhere from 4-24 hours depending of the type and structure of the glass and the extent of strengthening desired. The strength increase is dependent on two factors. First, the relative size of the ions “stuffed” into the glass compared to the ions exchanged out. In a typical sodium-containing glass, the sodium ions are exchanged for larger potassium ions. To do this, the glass is immersed into a molten ion bath at a temperature below the glass’s transition temperature, but higher than the melting point of the salt. Depending on the chemical interaction and immersion time, case depth can be varied from 30-40 microns to greater than 300 microns. Once the exchange process for strengthening the D-263 glass was more thoroughly understood, five slumped flat glass pieces (3.5” x 3.5”) along with three slumped shells were chemically strengthened for testing. Both types of glass samples were tested using the same processes used for earlier glass strength testing. The results from the testing are show in Figure 2.22

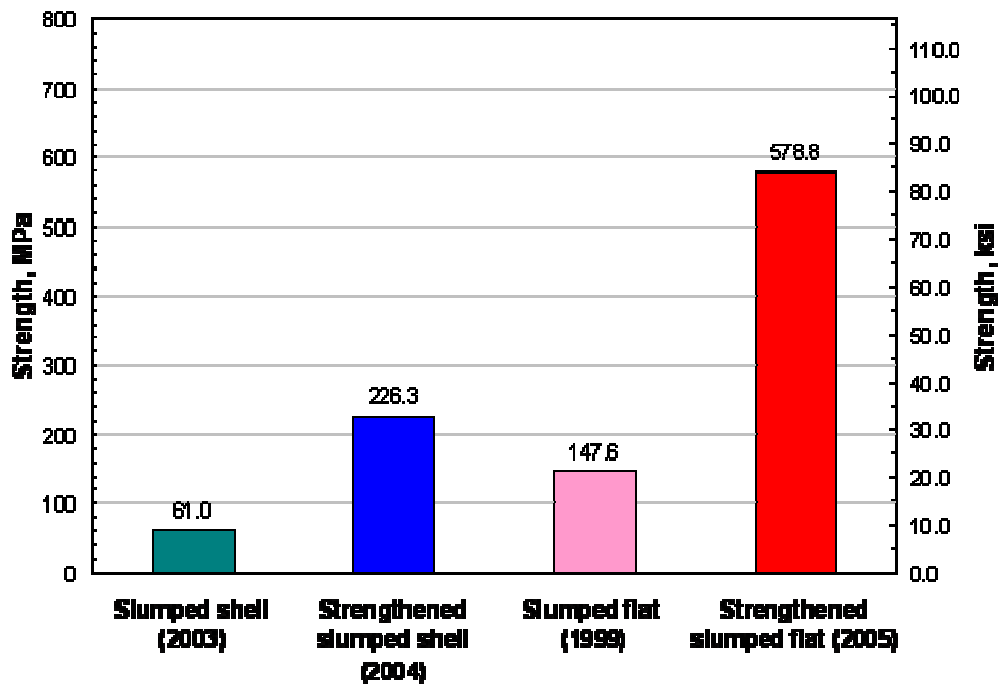


FIGURE 2.21: Strengthened D-263 Glass Strength Comparison [21]

Both of the glass sample types experienced significant growth in average strength. It is important to note that very few samples were tested compared to the sample sizes in earlier tests. Figure 2.22 presents the average strength data for the 1999 slumped flat pieces versus the strengthened slumped flat samples tested in 2005 and the slumped shell strengths from 2003 compared to the strengthened slumped shell samples. The ion exchange process strengthened the slumped shells by 271% and the slumped flat samples by 292%. The differences between strength increases are primarily attributed to edge defects that are considered in the bending test. All three glass shell samples fractured due to edge defects, resulting a fracture pattern similar to what is shown in Figure 2.23.

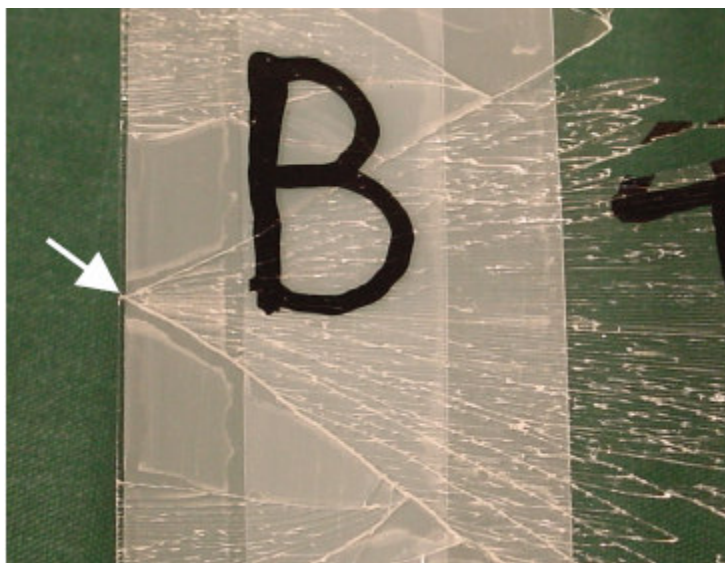


FIGURE 2.22: D-263 Failure Due to an Edge Defect

From the strength properties perspective, the ion exchange process is extremely promising.

Current testing with the ion exchange process is examining how the ion exchange affects on the glass shells shape at the submicron level due to the optical property requirements for the Constellation X SXT telescope.

### **2.10 Finite Element Modeling of Launch Loads**

The Constellation X team member Janet Squires developed a finite element model to predict the failure level of the glass shells. The model was based on the results of the strength testing on the slumped shells and flat pieces. The modeling was performed using NASTRAN on a glass shell held at five points on the top and at the bottom. She also used this model to predict the g level where the glass would fail during vibration testing.

The model is based on the observed average strength of 8.7 ksi for slumped glass shell reflectors. The current estimated launch loads are on the order of 25 gn. Additionally, NASA 5001 Standard requires that glass have a factor safety of three, or in this case, a load of 75 gn [18]. The FEA model used 8,481 elements and a total of 10,688 nodes. The 3 mil bondline is

included in the model while the glass shell was modeled with no gold or epoxy. The high factor of safety is required because of the scatter that is typically seen in strength data as a result of the unique properties of glass. Janet Squires' FEM indicated that the glass would not be able to meet this requirement.

## **2.11 Vibration Test 2004**

The vibration test that took place during 2004 had a similar goal as to this current vibration test. The need for vibration testing of the glass shells along with the surrounding mounting mechanism was realized early in the process of determining the strength characteristics of D-263 glass. Unfortunately, an initial vibration test plan centered on using the OAP2 housing with a mirror pair mounted was cancelled due to funding cuts. As a result, a less expensive plan was developed under the guidance of Andrew Carlson. This testing focused on using one glass shell mounted in titanium plates attached to the aluminum housing. A lower level vibration table was used in place of more capable shaker table than was planned. Analytical modeling was completed by Janet Squires to predict fundamental frequencies and failure point based on the available strength data for D-263 glass. Since many of the test articles and equipment was also used in the test that is the subject of this thesis, a more complete development of the FEA and mounting fixture can be found in Chapter 3.

The tested used NASA Goddard Space Flight Center code 543 Ling Dynamic Systems (LDS) Force Vibration Table, Model # 730-335B and a 48 digital vibration controller (DVC) with four channels. A picture of the LDS 730-335B is shown below in Figure 2.24 with the mounting plate attached. All four channels were used in the testing. One accelerometer was placed on the mounting plate, while the remaining three were placed on the mirror mount. Two of those were placed on the aluminum structure, one measured vertical acceleration and the

second measured horizon acceleration to ensure a consistent testing. The final accelerometer was placed on the titanium end plate to determine the behavior of the end plate relative to the aluminum structure. No accelerometers were placed on the glass shell to prevent premature failure of the glass. Figure 2.24 show the accelerometers in their actual locations.

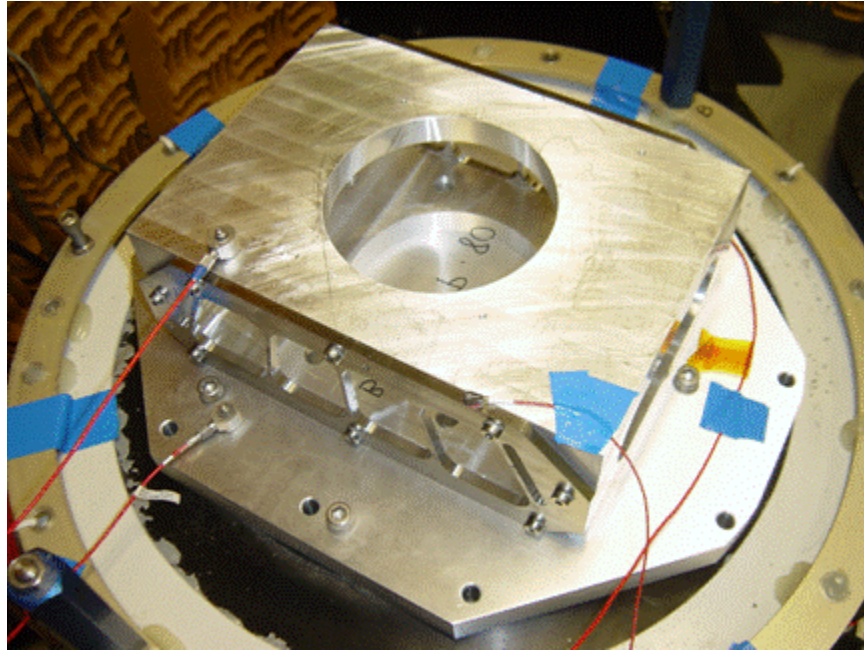


FIGURE 2.23: 2004 Vibration Setup [6]

Testing revealed that the first mode of the structure is at 600 Hz. Since no measurements were taken on the glass shell, the vibration analysis was unable to ascertain the first modal for the glass shell. Sine bursts tests were accomplished at 45.76 gn and 75.76 gn. The glass did not show any structural degradation from a visual inspection and survived a post-sine-burst sine sweep from 5-2000 Hz. Testing ended at 75.76 gn because this was the shaker table's limit with the weight of the mirror mount and structure. Figure 2.25 below shows the initial sine sweep with acceleration as a function of frequency. While the test did provide some useful data, it was apparent that an additional tests were needed with more capable equipment to gain a better understanding of the glass in the baseline mounting scheme.

### Post Sine Sweep-Acceleration as a Function of Frequency

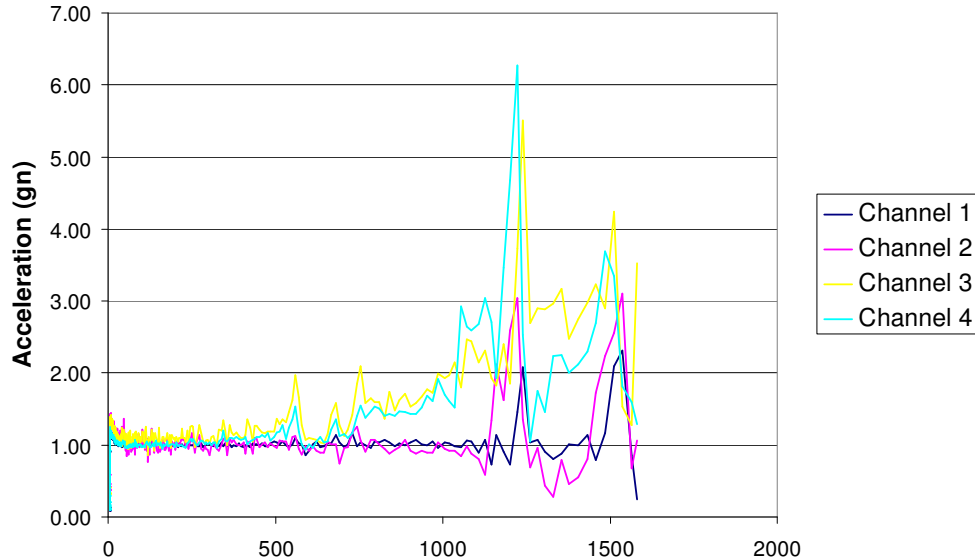


FIGURE 2.24:: Sine Sweep from 2004 Vibration Test [6]

## 2.12 Flight-Like Vibration Test

An initial vibration test plan was developed for OAP 2 for qualification. As previously discussed, the OAP 2 contained two mirrors, a parabolic and hyperbolic mirror from the 489 mm diameter. The goals of this particular test were:

- (1) Determine extent of glass mirror survivability
- (2) Perform sine sweep to determine structure modes
- (3) Perform pre/post test alignment check with ray tracing test fixture
- (4) Correlate OAP2 finite element model

It used Atlas 5 as the baseline qualification goals for this test. The test plan included a 3 axis sine burst and acceleration limited sine sweep test and 3-axis random vibration test. The total weight of the fixture with the mounting is 29.6 lbs. The planned sine sweep was from 5 Hz to 2000 Hz at 0.1 G. This test was very similar to the test performed by the author with a few

exceptions. First, the test examined not just the mounting technique, but also a fuller representation of the SXT mirror mounting hardware. -Second, the test included a two minute duration, three axis random vibration test. Otherwise, this test included many of the same goals as Carlson's 2004 test and this author's 2005 vibration test. Due to a reduction in funding, the test was cancelled which forced the Constellation X SXT team to develop a more economical test method with reduced goals.

Carlson's 2004 test was a first step in developing a low cost vibration test technique for the SXT mirrors. The results indicated that the fixture developed was suitable for future testing and provided data on the performance of one mirror. The test, however, was unable to validate the first modal of the mirror, nor were a sufficient number of mirrors tested to develop a statistical database of the mirror performance. It is also important to note that the shaker table reached a level of 75 gn's and the mirror did not break based on a visual inspection. This gn level is the upper limit of the particular shaker table used at the time.

After an in-depth review of the current literature on vibration testing, a few items were identified as important to any vibration test along with several different types of test. The three most prominent types of test are sine sweeps, sine or shock burst, and random vibration test. Each of these tests has an important role for any qualification role of spacecraft or other rocket launched hardware.

Using an equivalent loading method, the estimate input accelerations on the Constellation X SXT mirror are around 25 gn. This is primarily caused by vibration and acoustic loads during initial launch phase. Additional forces will be felt when the vehicle accelerates through the speed of sound and during spacecraft deployment. For Constellation X to be successful, the SXT mirrors cannot fail during launch or while on orbit. If even one mirror

fractures, it poses a serious threat to achieving the science that is vital to understanding the universe.

## **CHAPTER 3: PROBLEM STATEMENT**

### **3.1 Statement of Purpose**

The vibration test is focused on achieving four major goals. The 2004 test performed by Carlson, while useful, was unable to provide sufficient information to achieve the objectives.

Below is a discussion of the four objectives for this vibration testing:

- (1) Validation of the survivability of glass during launch loads. As previously discussed, the Constellation X telescopes will be launched on an Atlas V or Delta IV Heavy launch vehicle. Both of these vehicles create strong acoustic loads and structural loads during the initial launch and as they pass through Mach 1, approximately 1000 ft/sec.
- (2) Correlate the analytical model to actual test data. This is particularly valid for determining two pieces of information, failure load and natural frequency. Any time a finite element model is developed, it is always necessary to ensure that the model is accurate to actual tests. If the model matches the actual data, it ensures that the components used in the test are well understood (particularly the glass), if not, it indicates that there are areas that still require additional investigation to understand.
- (3) Understanding of D-263 glass properties under quasi-static loads. While the strength of the glass has been determined using ring-on-ring bi-axial tests and bending tests, additional tests simulating launch conditions are needed to determine the glass response and strength when mounted in this baseline scheme.
- (4) Develop a baseline method for comparison of future mounting designs of SXT mirrors. This test is the second of two tests performed on this mounting design in

order to gain an understanding of the impact of an adhesive bond between in D-263 and Epon 9394 structural adhesive in a titanium groove. In the past year, numerous other promising mounting techniques have been identified, but all rely on similar grooved interface between the mirror and titanium structure.

### **3.2 Test Matrix**

Testing is focused on three mirrors that have been mounted into the titanium struts and aluminum housing. Originally, four mirrors were going to be tested, however, one mirror failed during test preparation and handling, and thus removed from the test matrix. Vibration testing was accomplished using sine burst and sweeps. Since this testing is primarily interested in the strength of the glass in a vibration environment, no random testing will be done during this test. Table 3.1 presents the sine burst schedule for each mirror set. The vibration table is limited to a maximum of 50 gn due to the vibration fixture weight at 50 Hz. Therefore, after achieving this maximum, the remaining tests are performed at 90 Hz which provides the ability to increase the level up to 90 gn. The original testing plans called for a maximum level of a 100 gns, this was reduced to 90 gn due to resonance concerns within the vibration table. Mirror 489 P-80 was tested up to a 100 gn. The shaker table failed at the end of this particular test. To ensure that the vibration table would not fail again, the maximum gn level at 90 Hz was reduced from 100 gn to 90 gn for the remaining mirrors (489 P-88 and 489 P-90). The test plan, shown in Table 3.1, was also modified in a second way.

Table 3.1: Test Matrix for Vibration Test

<b>Fixture/ Mirror</b>	<b>Max G Level at 50 Hz</b>	<b>Drive Signal Levels at 50 Hz for 50 g's max (dBs)</b>	<b>Max G Level at 90 Hz</b>	<b>Drive Signal Levels (dBs) at 90 Hz for 100 g's max (dBs)</b>
489 P-80	50 g's	-6 (25 g's), -2 (40 g's), 0	100 g's	-6, -5, -4, -3, -2, -1, 0
489 P-90	50 g's (dependent on P-80)	-6 (25 g's), -2 (40 g's), 0	90 g's	-6, -5, -4, -3, -2, -1, 0
489 P-88	50 g's (dependent on P-80)	-6 (25 g's), -2 (40 g's), 0	90 g's	-6, -5, -4, -3, -2, -1, 0

When the plan was developed, the Constellation X team was unsure of how the mirrors would perform. If the first mirror survived up to 90 gn, the remaining mirrors were to be tested only using the 90 Hz test schedule. While mirror 489 P-80 survived 100 gn, the mechanical failure of the vibration table prevented a post sine sweep from occurring. Due to this problem, the glass shell 489 P-90 was tested using both the 50 Hz and 90 Hz test schedule followed by a sine sweep. After the data showed that this glass shell survived the sine burst, the remaining glass shell, was only tested at the higher frequency sine burst.

Besides a series of sine bursts, a sine sweep was performed before any sine burst and between frequency adjustments of 50 Hz and 90 Hz. These sine sweeps ensured that all hardware is secure on the vibration fixture, and in combination with the laser vibrometer, that the glass has not sustained critical damage. The sine sweeps are performed from 10-2000 Hz at 0.1 gn. The low acceleration value is used to ensure that the test article will not fail during sine sweep when resonance frequencies are reached. Resonance frequencies typically defined as when the forcing frequency (vibration table) is at or near the value of the natural frequency of the structure.

### 3.3 Vibration Testing Equipment and Setup

The vibration testing relied on the same fixture designed for the 2004 vibration test. This fixture is light weight, but still has sufficiently accurate characteristics to ensure that data

gained from this experiment is valid. The design of the vibration fixture was accomplished by the work of several Constellation-X team members including Bobby Nannan (Swale), Janet Squires (Swale), and Andrew Carlson (USAF). The full vibration fixture is shown in Figure 3.1.

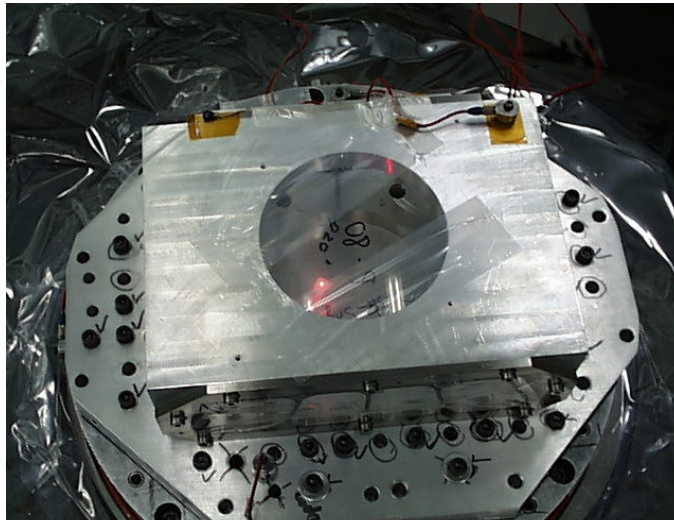


FIGURE 3.1: Vibration Fixture and Housing

The fixture is attached to an aluminum plate that serves as an interface between the housing unit and the vibration table. It is milled out of aluminum and holes are drilled to match the bolt pattern for the vibration table. The weight of the vibration plate is 18.89 lbs. The aluminum housing performs the role as a cheap OAP module. It is also made out of aluminum to reduce costs and weighs 12.25 lbs. A critical component for flight like accuracy in this test is the interface between the mirror and load bearing structure. In this case, it is the titanium strut plates that are very similar to the OAP2 struts. As previously discussed, almost all designs evaluations have the mirrors mounted in a titanium groove similar to what is seen on this vibration fixture. The titanium plates are attached using hex bolts and weigh 1.71 lbs while the mirror is attached to the titanium by epoxy in a 3 mil groove. Titanium was used for the struts for several reasons. Besides being more representative of the current designs, titanium also possesses a much lower

CTE value. This lower CTE value prevents additional stresses from being introduced into the mirror through temperature changes.

This testing used the Ling B-335 vibration exciter. This shaker is operated by Code 549-NASA Goddard Space Flight Center in the Structural Dynamics Test Engineering under Environmental Test Engineering and Integration Code 549. It has a maximum force rating of 17,500 lb for sine burst while a 12,000 lb random rms limit. It is also capable of varying the frequency from 5 Hz to 2000 Hz. The digital vibration control system used is able to process up to 4 accelerometer signals and control based on the minimum, maximum, rms, or average of the signals. For safety, a redundant accelerometer is always connected to a Unholtz-Dickie 123 vibration monitor limiter. This provides a safety to ensure that displacement or acceleration limits are not exceeded.

Another critical piece of testing equipment is the Ometron VS 1000 Laser Vibrometer. This system sits above the shaker table and lasezes a target placed on the mirror. A portion of the laser light is then reflected back to the detector on the VS 1000. The reflected light wave is then compared against the reference beam to determine the velocity of the structure. It is capable of working up to 20 meters away in optimum conditions. The maximum velocity that the VS 1000 is capable of detecting is 1000 mm/sec or about 40 in/sec [19].

The primary role of the laser vibrometer is to measure the response of the glass shell during testing. In the previous 2004 vibration test, no data was taken from the mirror so there was no way to confirm the predicted FEM by Janet Squires of a first modal at 168 Hz. A secondary role is to help detect the failure load of mirror, since a change in the structure of the mirror should be readily apparent in the laser vibrometer data, assuming that velocity seen is below the limits of the VS 1000. Due to the fixture style and position of the mirror in housing,

the VS 1000 was set up above the shaker table while shooting the laser through the front window on to the glass shell as shown in Figure 3.2. Since the glass shell is transparent, a target is affixed to the surface, near the center of the mirror. The red dot shown in figure 3.2 is the location of the laser beam on the target in the mirror housing.

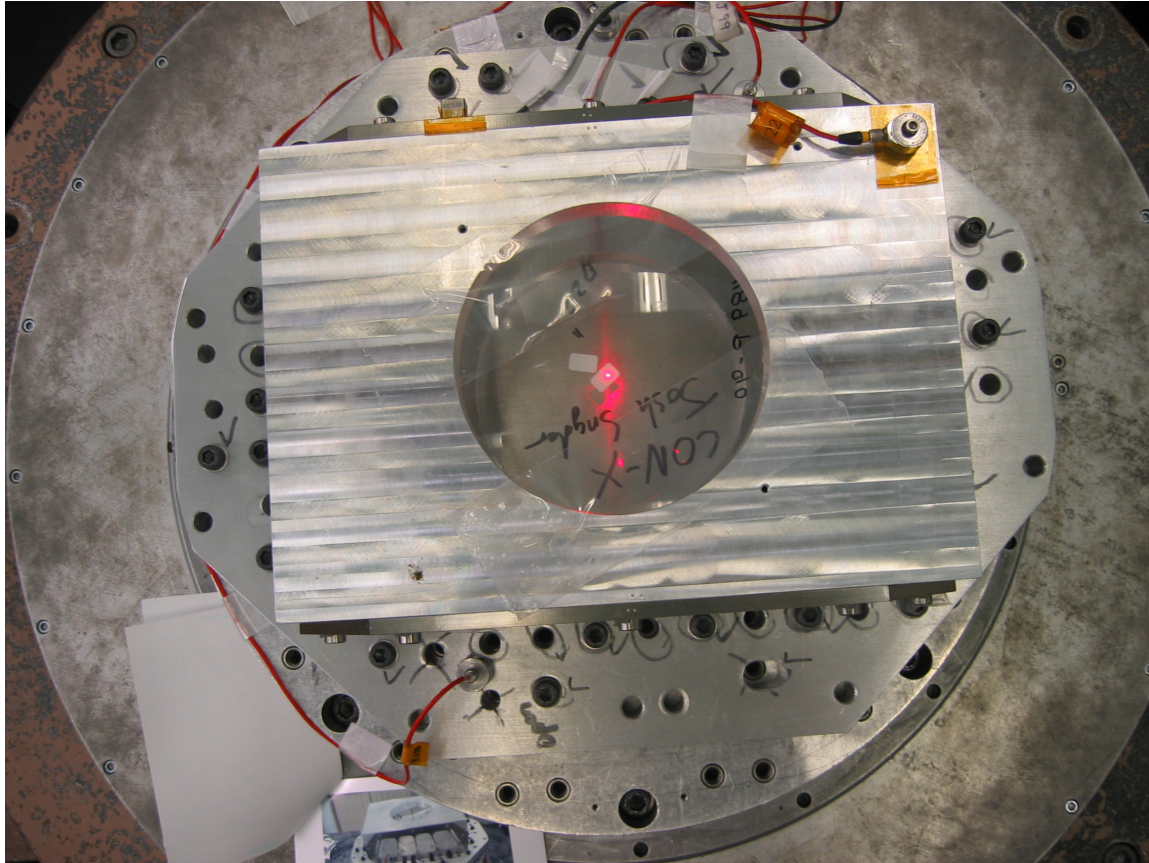


FIGURE 3.2: Laser Vibrometer Measurement Position on Mirror

In combination with the laser vibrometer, two accelerometers were used. The locations of the accelerometers were very close to the locations for the 2004 vibration test, and used the same type of the accelerometers. A single axis accelerometer, Endevco 2221D, was placed on the top of the aluminum fixture, while a tri-axis accelerometer, Kistler 8791, was placed on the titanium plate on the side of the fixture. The accelerometers were positioned such as to provide

information on the role behavior of the aluminum fixture and the titanium strut end plates compared to the behavior of the mirror as shown in Figure 3.3

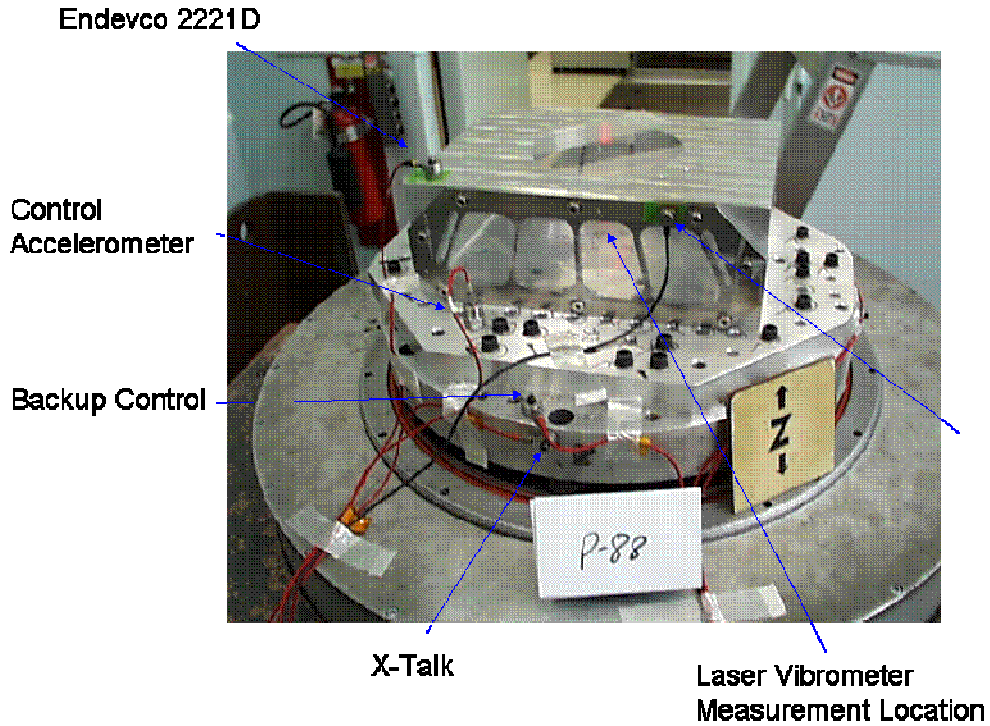


FIGURE 3.3: Accelerometer Positions

### 3.4 Finite Element Analysis Modeling

Janet Squiries of Swales Aerospace performed a finite element analysis of the complete test article in 2005. This model was used in several ways including predicting resonance frequencies and the failure load for the glass shell. The model included 8,481 elements and 10,688 nodes. All components of the test article were modeled including the adapter plate, housing, titanium strut plates with a 3 mil bond, and a glass reflector without gold or epoxy. Figure 3.4 shows the full finite element model for the test article.

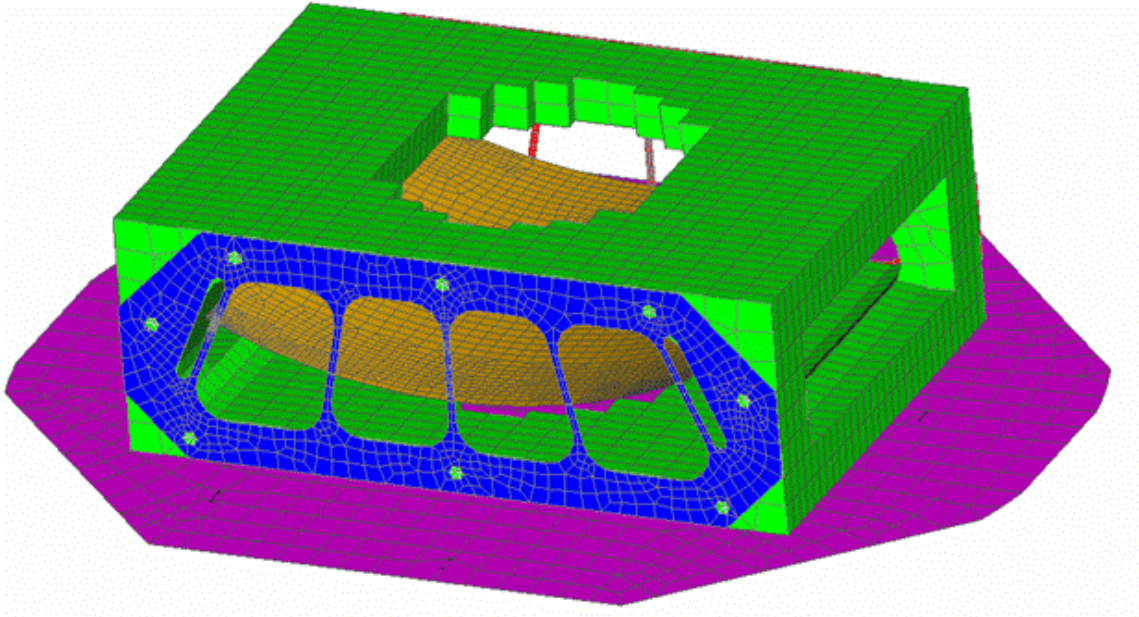


FIGURE 3.4: Finite Element Model [20]

Using this model, the first mode of the reflector was determined to be at 168 Hz. A depiction of the mirrors behavior when vibrated at this frequency is shown below in Figure 3.5. The second mode of the glass shell was determined to be at 175 Hz. The first mode of the complete test article is expected to be around 600 Hz as seen in Carlson's 2004 Vibration test.

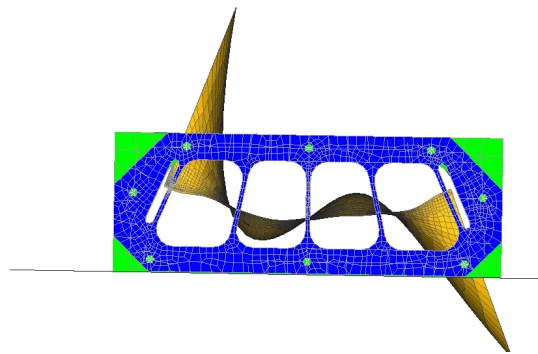


FIGURE 3.5: First Mode Prediction from FEA Model at 168 Hz

Squires also predicted the failure of the glass shell to occur at 46.2 gn based on a glass strength of 8.5 ksi observed from the earlier glass shell testing. This assumes that no crack growth takes place during build up tests to the higher loads. It is possible that lower level sine

burst or the sine sweep at the resonance frequency of the glass may cause sub-critical crack sizes to grow to such a level that glass shell fails at a lower than predicted level.

The maximum stress in the model occurs where the glass shell is bonded in the titanium groove. Since this bond area is small, these locations act like point loads. Additionally, the outer edge of the four outer struts appear to cause a significantly higher stress than the other struts due to their outer location as shown in Figure 3.6 below.

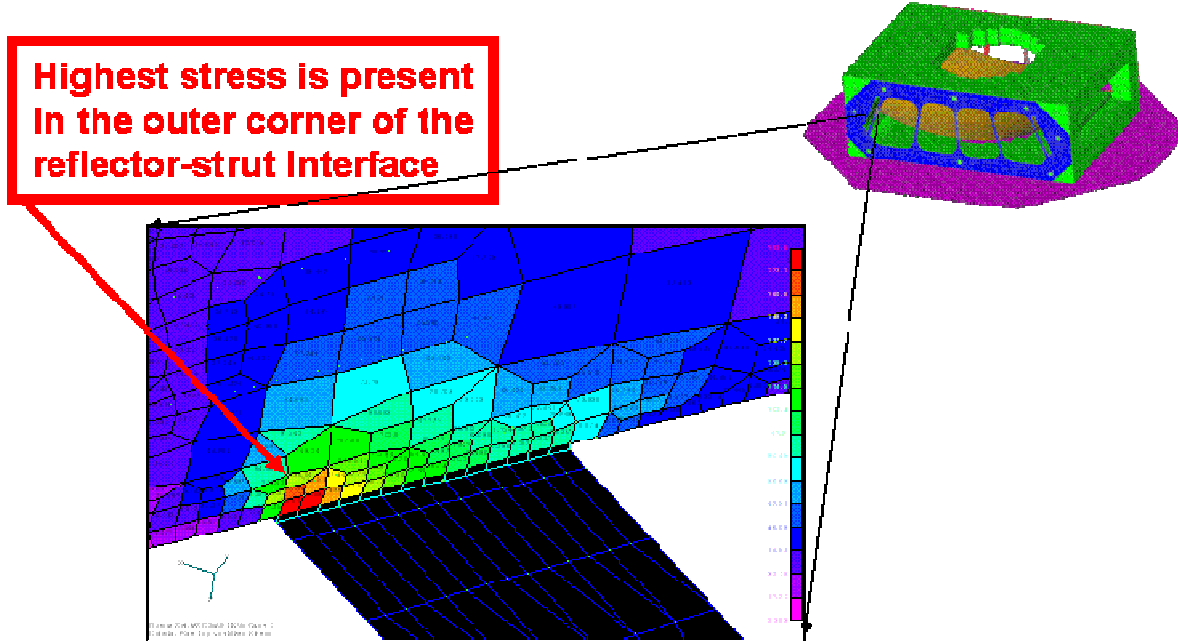


FIGURE 3.6: FEA Model Prediction of Highest Stress

## CHAPTER 4: RESULTS AND ANALYSIS

All three mirrors were successfully tested and survived at least 90 gn and data from the response measurements, including the laser vibrometer data, is consistent. The three mirrors showed no indications of fatigue or other damage during post sine bursts evaluations. The finite element model accurately predicted the first mode of the mirrors in this configuration at 168 Hz, but the model did not accurately predict the failure level of the mirrors. All mirrors survived almost two times the predicted failure load from the FE model of 46.2 gn. Mirror 489 P-80 survived the maximum load seen by any of the mirrors, 106 gn. Due to some minor differences between the tests, each mirror is individually discussed followed by a comprehensive overview of the data from the testing. The typical full level sine burst is shown below in Figure 4.1.

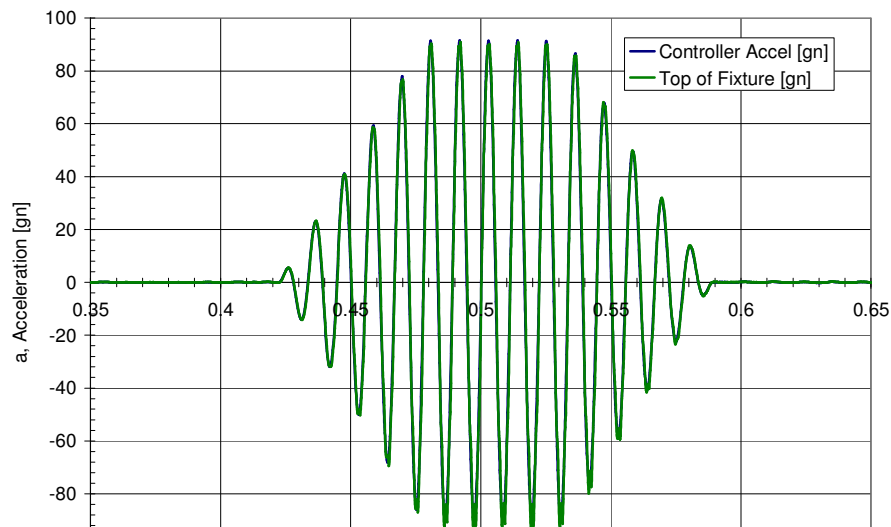


FIGURE 4.1: Typical Sine Burst Response for the Sine Burst Tests

#### **4.1 Mirror 489 P-80**

This mirror was the first of the three tested. This mirror was tested at 50 Hz up to 50 gn and at 90 Hz up to 100 gn goal. The mirror actually hit a maximum level of 106. Midway through this full load test at 100 gn, the vibration table armature failed. This prevented a post sine sweep to provide further information if the mirror failed during the testing. A sine sweep was performed before testing and between the 50 Hz and 90 Hz tests. A visual inspection of the mirror after the 100 gn abort test show no indications of fatigue or failure. The first mode of the mirror is seen at 168 Hz, consistent with the FE model predictions. It is difficult to distinguish if the prediction of a second modal at 175 Hz is accurate. The laser vibrometer data did clearly show a mode at 400 Hz.

#### **4.2 Mirror 489 P-90**

Mirror 489 P-90 was tested up to 90 gn and completed three sine sweeps (prior to testing, between 50 Hz and 90 Hz testing, and post testing). This was the first of the two mirrors tested after the vibration table failure. This mirror, like all other mirrors, was first subjected to a 0.1 gn sine sweep from 10-2000 Hz. The laser vibrometer data did show a first modal around 168 Hz, consistent with the FEM predictions. The mirror was successfully tested at 50 Hz to a maximum acceleration of 50 gn. The sine sweep that was performed before moving to 90 Hz did not show any indications that the mirror weakened due to the testing. The 90 Hz was also completed successfully along with the a post test sine sweep.

#### **4.3 Mirror 489 P-88**

Mirror 489 P-88 completed sine burst testing at 90 Hz and a pre and post sine sweeps. Since all earlier mirrors survived at least 50 gn, 489 P-88 skipped all 50 Hz testing and was only

tested at the 90 Hz levels. The results from Mirror 489 P-88 are consistent with the other three mirrors. The post sine sweep did not indicate any structure degradation of the structure or the mirror.

#### 4.4 Mirror Comparison

All three mirrors showed a very similar behavior throughout the sine sweep frequencies. Each mirror showed a resonance frequency at approximately 168-174 Hz, consistent with the expectations from the FEA model. A comparison of the sine sweeps performed before testing and after testing is shown below in Figure 4.2.

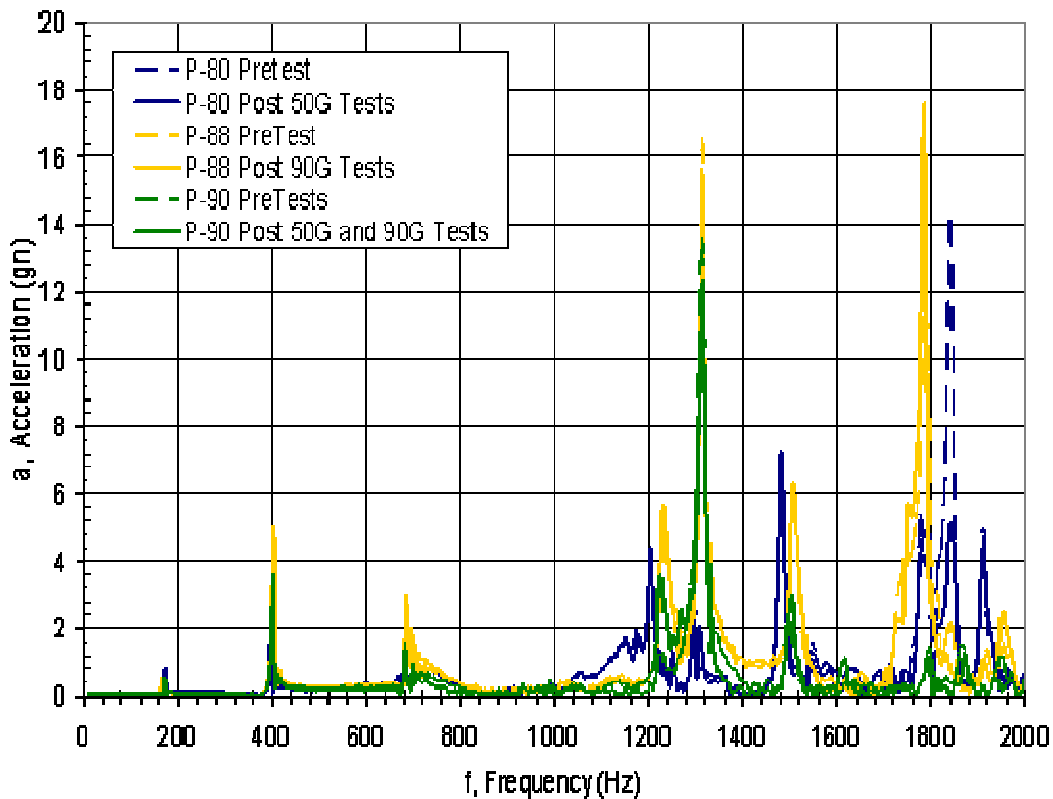


FIGURE 4.2: Pre and Post Sine Sweep Comparison

The data for all four mirrors indicate only minor changes in the resonance frequencies of the mirrors. There is no indication of significant fatigue or structural degradation of the fixtures or mirrors. It is difficult to determine the precise resonance frequencies of the mirrors. There was a

small variance of the peak acceleration and frequency of the resonance between the mirrors. This indicates that there was some variance in the bond quality between the three different fixture/mirror sets. Figure 4.3 shows a detailed picture of the mirror responses at and near the resonance frequencies.

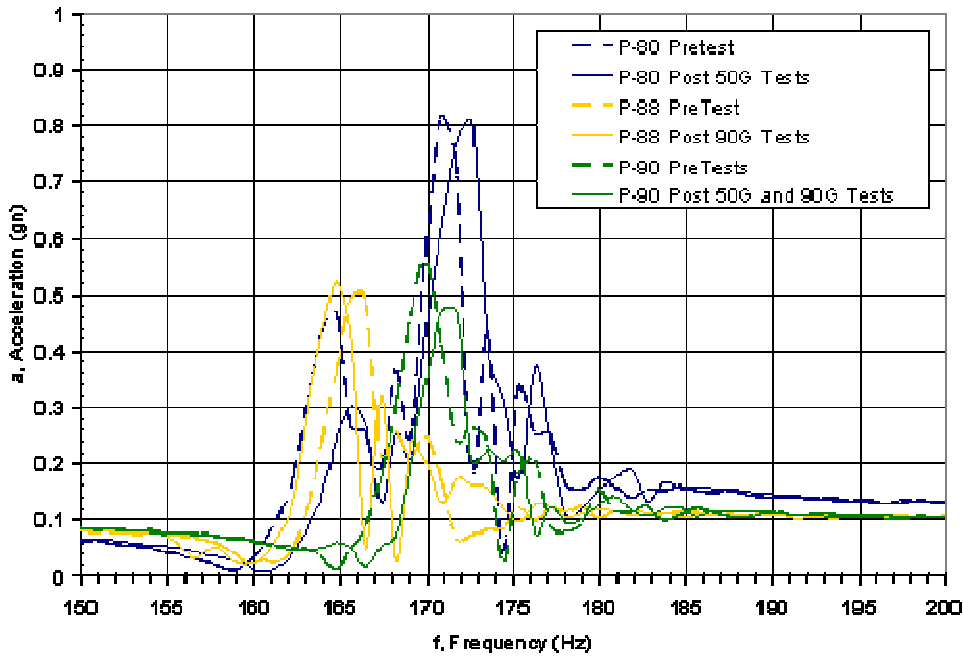


FIGURE 4.3: Sine Sweep Data at First Resonance Frequency

Surprisingly, the data also indicated a second mode at 400 Hz. This was seen in all mirror sine sweeps, but was not predicted during of the pre-testing analysis. Additionally, this mode was not driven by the fixture response to the vibration excitation. The resonance at 400 Hz appears to be significant due to the level of response, seen in Figure 4.4, and should be investigated further to determine if this poses a risk to the mirrors during launch.

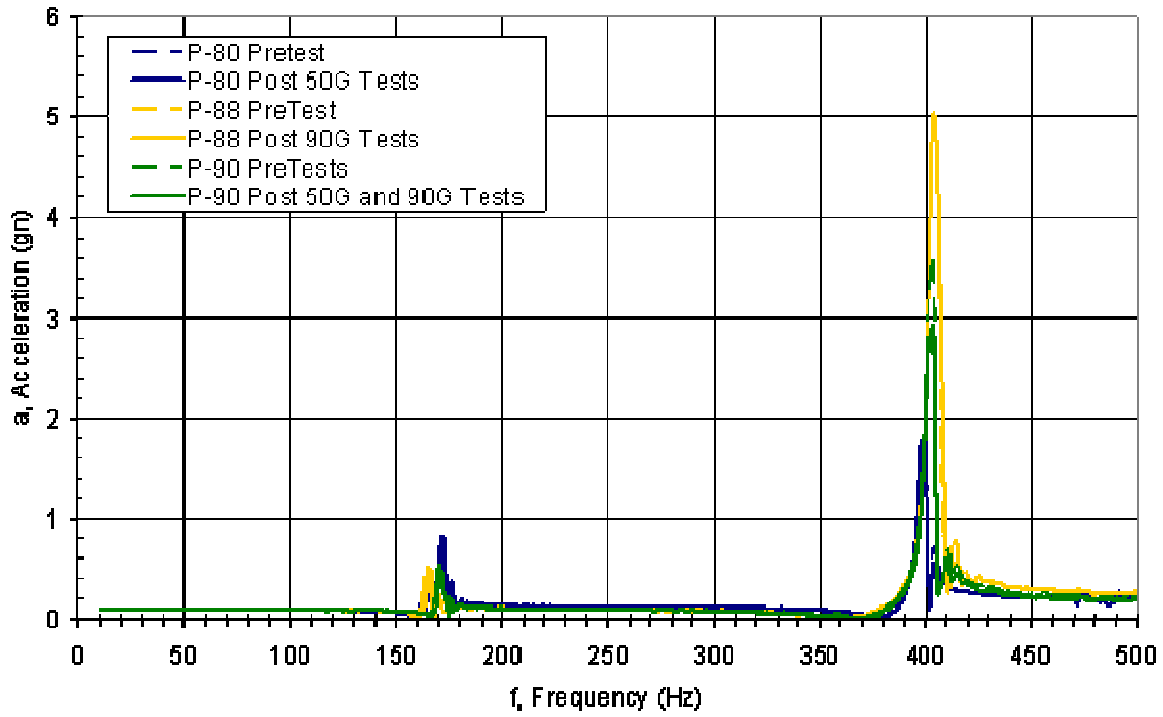


FIGURE 4.4: Sine Sweep Response over 10-500 Hz for All Mirrors

## **CHAPTER 5: CONCLUSIONS AND RECOMMENDATIONS**

The vibration testing of three Constellation X glass substrates mounted in a titanium grooves was extremely successful. The testing provided critical understanding of the D-263 glass strength while subjected to high level vibration loads and resonance frequencies when mounted in a 10 titanium mount. The data from this testing indicates that the Schott D-263 glass meets the requirements for glass set forth in the NASA Standard 5001. Once the configuration is finalized along with the launch vehicle, additional testing may needed. This testing, however, enables the Constellation X team to focus on other areas.

All four objectives were achieved from this testing. As previous mentioned, the FEM successfully correlated the natural frequency of the mirror during sine sweeps. The FEM did not accurately predict the failure load of the glass. This is not completely surprising for several reasons. First, predicting strength of glassy materials is difficult because of the defects that can be present on the surface and along the edge of the mirror, particularly near the attachment points. Second, the testing that produced the estimates for the mirror failure loads was based on a much lower rate of load application than seen during vibration testing. Despite these difficulties with FEM, this testing can be used to further enhance the accuracy of the model as the Constellation X telescope moves toward flight status.

The results from this series of test indicate that the mirrors are capable of surviving the vibration launch loads. NASA requires that glass be certified of surviving three times the expected loads when used in any satellite. The mirrors clearly exceeded this requirement and do not represent any major hindrance for use in the SXT Constellation X telescope.

This was the first testing of Schott D-263 glass under vibration loads while being monitored by a laser vibrometer. The laser vibrometer enabled the Con-X team to determine the resonance frequencies of the mirror and provided a mechanism to determine if any significant growth in crack size had occurred. This testing is also most comprehensive evaluation of the glass performance when mounted in the baseline fixture for the SXT telescope. The data from these “baseline fixture” vibration tests will form the basis of evaluation for future design.

Despite the success of these tests, there are several areas that should be further pursued, particularly with regards to glass strength. First, the critical crack size for the D-263 glass needs to be determined when mounted and the nominal crack size throughout processing. This will provide a way to measure crack growth throughout the life of the mirror during a variety of tests. It will also give a better understanding of the expected life of the mirror when mounted in a stressed position. Second, while the glass will survive the vibration loads generated during launch, additional testing should be performed to evaluate the performance when several mirrors are located within close proximity and subjected to acoustic loads which are also present during launch. A method of proof-testing the glass also needs to be developed to ensure all of the mirrors on the flight Constellation X SXT will survive to the end of the telescopes life. If one mirror breaks during launch or operations, the shards will reflect the X-rays within the telescope, rendering the SXT useless. The design of this proof test will be difficult because the test needs to ensure that the mirror will not break from launch to end of operations, while not causing crack growth that will act as the basis of a future failure of the glass. In all of these future tests, a much higher number of samples should be used. This test only used three due to cost constraints, but given the time and funding at a later stage in the program, additional samples should be attained for testing.

This vibration testing was extremely successful. All four of the objectives were met and the glass performed to a higher level than predicted. There are several areas where additional scrutiny is needed before the mirrors can be declared ready for flight, however, the greatest step has been achieved by showing that the mirrors are capable of surviving high acceleration rates when mounted in titanium groove bonded by epoxy.

## REFERENCES

- [1] Official NASA Constellation-X Home Page. Greenbelt, Maryland: NASA Goddard Space Flight Center. 1 Sept 2004. < <http://constellation.gsfc.nasa.gov/>>.
- [2] Thompson, William T. Theory of Vibration with Application. New York: Prentice Hall, 1997.
- [3] Sine-Burst Load Test. Practice No. PT-TE-1420. Greenbelt, Maryland: NASA Goddard Space Flight Center.
- [4] Varshneya, Arun K. Fundamentals of Inorganic Glasses. San Diego: Academic Press, Inc., 1994.
- [5] Uhlmann, D.R. and N. J. Kreidl, ed. Glass: Science and Technology: Elasticity and Strength in Glasses. New York: Academic Press, 1980.
- [6] Carlson, Andrew. Vibration Testing of the NASA Constellation X Spectroscopy X-Ray Telescope Reflectors. Washington, DC: George Washington University, 24 September 2004.
- [7] Constellation X-Ray Observatory: Unlocking the Mysteries of Black Holes, Dark Matter, Dark Energy, and Life Cycles of Matter in the Universe. Greenbelt, MD: NASA Goddard and Smithsonian Astrophysical Observatory, 2004.
- [8] "Reference Design". Constellation X Science Site Mission Design. Greenbelt, MD: NASA Goddard Space Flight Center. 1 Sept 2004.  
<[http://constellation.gsfc.nasa.gov/science/design/sc\\_configuration.html](http://constellation.gsfc.nasa.gov/science/design/sc_configuration.html)>.
- [9] "Trip Report Images." Constellation XRay (conx) Project Office Home. Greenbelt, MD: Project Office Goddard Space Flight Center. < <https://conxproj.gsfc.nasa.gov>

/resources/image\_gallery/trip/page.asp?base=resources/image\_gallery/trip&target=index  
>.

- [10] Podgorski, William. Constellation X Spectroscopy X-ray Telescope Alignment. SPIE Proceedings Vol. 4851, 2002.
- [11] Petre, Robert and et al. The Constellation X Spectroscopy X-Ray Telescope. SPIE Proceedings Vol. 5488, 2004.
- [12] Squires, Burt. SXT Technical Interchange Meeting (TIM) Reflector Strength and Alignment. 10 Dec 2003.
- [13] Hair, Jason. Constellation-X Soft X-Ray Telescope Segmented Optic Assembly and Alignment Implementation. SPIE Proceedings Vol 4581, 2002.
- [14] Owens, Scott, et. al. The Constellation-X SXT Optical Alignment Pathfinder 2 Design, Implementation and Alignment. SPIE Proceedings Vol 5168, 2004.
- [15] Schott North America. <<http://www.schott.com/fpd/english/products/fpd/d263t.html#main>>. 2003.
- [16] He, Charles and Len Wang. Constellation-X Glass Strength Investigation: Strength Variation among Deliveries and Effect of Cleaning on Strength. Greenbelt, MD: NASA GSFC Code 541, 21 June 2004.
- [17] Varshneya, Arun and William C. LaCourse. "Technology of Ion Exchange Strengthening of Glass: A Review." Ceramic Transactions, Vol 29, American Ceramic Society, Westerville, OH, 1993, pg 365-78.
- [18] NASA Technical Standard 5001.
- [19] Ometron VS 100 Operator's Manual. Issue 4, October 1995.
- [20] Squires, Janet. Constellation X SXT Reflector Vibration Analysis. 17 Aug 2004.

[21] He, Charles and Len Wng. Strength of Chemically Strengthened Slumped Glass Shells and Flats. Greenbelt, MD: NASA GSFC Code 541, 9 Feb 2005.

[22] He, Charles and Len Wng. Constellation X Strength Investigation: Effects of Slumping on Glass. Greenbelt, MD: NASA GSFC Code 541, 5 May 2005.

[23] He, Charles and Len Wng. Strength of Slumped Glass Shells for Constellation X. Greenbelt, MD: NASA GSFC Code 541, 17 Dec 2003.